

1 **Chemical characterization of organic vapors from wood,** 2 **straw, cow dung, and coal burning**

3 Tiantian Wang¹, Jun Zhang¹, Houssni Lamkaddam¹, Kun Li^{1, a}, Ka Yuen Cheung¹, Lisa
4 Kattner¹, Erlend Gammelsæter^{1, b}, Michael Bauer¹, Zachary C.J. Decker^{1, c, d}, Deepika Bhattu²,
5 Rujin Huang³, Rob L. Modini¹, Jay G. Slowik¹, Imad El Haddad¹, Andre S. H. Prevot^{1, *}, David
6 M. Bell^{1, *}

7 1 Laboratory of Atmospheric Chemistry, Paul Scherrer Institute, Villigen, 5232, Switzerland

8 2 Department of Civil and Infrastructure Engineering, Indian Institute of Technology Jodhpur, 342037, India

9 3 Institute of Earth Environment, Chinese Academy of Sciences, Xian 710061, China

10 a now at: Environmental Research Institute, Shandong University, Qingdao, 266237, China

11 b now at: Department of Chemistry, Norwegian University of Science and Technology, Trondheim, 7491, Norway

12 c now at: NOAA Chemical Sciences Laboratory (CSL), Boulder, CO 80305, USA

13 d now at: Cooperative Institute for Research in Environmental Sciences, University of Colorado Boulder, Boulder,
14 CO 80309, USA

15 Correspondence to: Andre S. H. Prevot (andre.prevot@psi.ch) and David M. Bell (david.bell@psi.ch)

16 **Abstract**

17 Solid fuel (SF) combustions, including coal and biomass, are important sources of pollutants in the
18 particle and gas phase and therefore have significant implications for air quality, climate, and human
19 health. In this study, we systematically examined gas-phase emissions using the Vocus proton-transfer-
20 reaction time-of-flight mass spectrometer, from a variety of solid fuels, including beech logs,
21 spruce/pine logs, spruce/pine branches and needles, straw, cow dung, and coal. The average emission
22 factors (EFs) for organic vapors ranged from 4.8 to 74.2 g kg⁻¹, depending on the combustion phases
23 and solid fuel types. Despite slight differences in modified combustion efficiency (MCE) for some
24 experiments, increasing EFs for organic vapors were observed with lower MCE. The relative
25 contribution of different classes showed large similarities between the combustion phases in beech logs
26 stove burning, relative to the large change in EFs observed. The C_xH_yO_z family is the most abundant
27 group of the organic vapor emitted from all SF combustion. However, among these SF combustions, a
28 greater contribution of nitrogen-containing species and C_xH_y families (related to polycyclic aromatic
29 hydrocarbons) is observed in the organic vapors from cow dung burning and coal burning, respectively.
30 Intermediate volatility organic compounds (IVOCs) constituted a significant fraction of emissions in
31 solid fuel combustion, ranging from 12.6% to 39.3%. This was particularly notable in the combustion
32 of spruce/pine branches and needles (39.3%) and coal (31.1%). Using the Mann-Whitney U test on the
33 studied fuels, we identified specific potential new markers for these fuels based on the Vocus
34 measurements. The product from pyrolysis of coniferyl-type lignin and the extract of cedar pine needle
35 were identified as markers in the spruce/pine branches and needles open burning (e.g., C₁₀H₁₄O₂,
36 C₁₁H₁₄O₂, C₁₀H₁₀O₂). The product (C₉H₁₂O) from the pyrolysis of beech lignin was identified as the
37 potential new marker for beech log stove burning. Many series of nitrogen-containing homologues (e.g.,

38 $C_{10}H_{11-21}NO$, $C_{12}H_{11-21}N$, $C_{11}H_{11-23}NO$ and $C_{15}H_{15-31}N$) and nitrogen-containing species (e.g.,
39 acetonitrile, acrylonitrile, propanenitrile, methylpentanenitrile) were specifically identified in cow dung
40 burning emissions. Polycyclic aromatic hydrocarbons (PAHs) with 9-12 carbons were identified with
41 significantly higher abundance from coal burning compared to emissions from other studied fuels. The
42 composition of these organic vapors reflects the burned solid fuel types and can help constrain emissions
43 of solid fuel burning in regional models.

44 **Keywords:** Vocus, solid fuel, primary emission, potential markers, combustion phase

45 **1 Introduction**

46 Solid fuels (SFs), including coal and biomass, are a primary source of domestic heating worldwide (Tao
47 et al., 2018; Oberschelp et al., 2019; Wu et al., 2022). In developing regions, such as India, more than
48 80% of rural households use biomass as cooking fuel (Balakrishnan et al., 2011). Firewood is mainly
49 used for rural households, followed by crop residues and cow dung ‘cakes’, which are made of a mixture
50 of dried cow dung and crop residues (Loebel Roson et al., 2021; Chandramouli and General, 2011). In
51 Europe, fireplaces and woodstoves are used for domestic heating in winter, which have considerable
52 impacts on air quality, resulting in intense ‘smog’ events (Kalogridis et al., 2018; Fourtziou et al., 2017;
53 Bailey et al., 2019; Font et al., 2022). China is the largest producer and consumer of coal in the world.
54 In China and some Eastern European countries like Poland, coal is widely used for domestic purposes,
55 such as heating and cooking of households, due to its cost-effectiveness and easy accessibility (Guo et
56 al., 2021; Stala-Szlugaj, 2018). The combustion of these solid fuels has been recognized as the main
57 source of anthropogenic emission of atmospheric pollutants that elicit adverse effects on air quality and
58 human health (Wu et al., 2022; Zhang and Smith, 2007).

59 Wildfires or bushfires have become more frequent in many regions due to heatwaves and drought
60 (Weber and Yadav, 2020; Williams et al., 2012). SF combustion, including wildfires, is a major source
61 of organic vapors to the atmosphere, emitting hundreds to thousands of different organic gas-phase
62 species (Hatch et al., 2019; Koss et al., 2018; Permar et al., 2021). Once emitted, evaporated vapors or
63 freshly emitted burning organic vapors will oxidize to produce oxygenated organic vapors with a broad
64 volatility range. These organic vapors with sufficiently low volatility will nucleate or condense onto
65 pre-existing aerosols to form secondary organic aerosols (SOA) (Kumar et al., 2023).

66 The identification of potential markers for each emission source will be highly valuable in evaluating
67 SOA formation potential and ambient source contributions. Liu et al. (2008) identified potential volatile
68 organic markers for different emission sources (e.g., biomass burning (BB), mobile sources and
69 painting). Nevertheless, these commonly used potential markers are well-established, yet due to their
70 presence in more than one type of biomass fuel, distinguishing between different biomass-burning
71 sources presents challenges. Since 2009, there have been many advancements in the gas-phase
72 measurements of SF, which include lab studies (Bruns et al., 2017; Bruns et al., 2016; Bhattu et al.,
73 2019) and large field campaigns (e.g., WE-CAN Aircraft Measurements, FIREX-AQ campaign)
74 (Permar et al., 2021; Jin et al., 2023; Majluf et al., 2022). However, efforts toward understanding SOA
75 formation in burning plumes have been hindered by limited identification and quantification of organic
76 vapors emitted by fires, especially intermediate volatility organic compounds (IVOCs) (Akagi et al.,
77 2011). Laboratory and field campaigns suggest that intermediate volatility organic compounds are

78 important precursors of SOA. Grieshop et al. (2009) demonstrated that traditional SOA precursors
79 account for less than 20% of the observed SOA formed from residential wood combustion emissions,
80 while IVOCs can contribute approximately 70% of the formed SOA (Li et al., 2024), which highlights
81 the urgent need for more research on IVOCs from BB emissions. Adding an IVOC emission inventory
82 to an air quality model can significantly narrow the gap between the estimated and measured SOA
83 concentrations(Li et al., 2024; Hodzic et al., 2010; Zhao et al., 2016; Robinson et al., 2007).

84 Offline sampling methods such as canisters and adsorption-thermal desorption (ATD) cartridges, along
85 with gas chromatography (GC) analysis, have limitations related to their low time resolution,
86 susceptibility to sampling artifacts, and a limited range of measurable compounds (Hatch et al., 2018;
87 Hatch et al., 2017). In addition to offline techniques, proton-transfer-reaction mass spectrometry (PTR-
88 MS) has been widely used for the online measurement of volatile organic compounds (VOCs) in the
89 atmosphere (Yuan et al., 2017). However, IVOCs still suffer from high losses in the sampling lines and
90 PTR-MS drift tubes. Furthermore, most studies have focused on either primary or aged emissions, with
91 very few examining the real-time influence of combustion conditions on the composition of emitted
92 organic vapors (Bruns et al., 2016; Akherati et al., 2020; Tkacik et al., 2017). The recently developed
93 Vocus PTR-TOF (hereafter Vocus) has greatly enhanced sensitivity due to a newly designed chemical
94 ionization source (Krechmer et al., 2018), and it can detect a broader spectrum of VOCs, IVOCs, and
95 their oxygenated products (up to six to eight oxygen atoms for monoterpene oxidation products) (Li et
96 al., 2020; Wang et al., 2021; Riva et al., 2019). With a novel design and chemical ionization source, the
97 Vocus allows for real-time characterization of gas-phase emissions during various burning phases (e.g.,
98 flaming and non-flaming phases) and identifies the potential markers for a wide range of fuels.

99 The present study compares real-time emissions from different combustion fuels. We begin by
100 demonstrating the evolution of gas-phase emissions during burning cycles highlight the changes in the
101 composition of the emissions. Then, we systematically characterize the organic vapors composition
102 using Vocus from a variety of burning fuels from both residential stoves (beech logs, spruce/pine logs,
103 and coal) and open combustion (spruce/pine branches and needles, straw, cow dung). We evaluate the
104 potential markers and EFs for different fuels and explore the dependence of individual organic vapor
105 emission intensity, variability, and chemical composition on solid fuel types and combustion phases.
106 We also discuss potential markers for the burning fuels examined in this study. The potential markers
107 are identified as statistical outliers determined with a Mann-Whitney test, consistent with previous
108 measurements (Zhang et al., 2023). The differences in EFs and profiles between different combustibles
109 can be considerable, and these results illustrate the importance of considering these emission sources
110 individually. Measurements capable of identifying and quantifying rarely measured and presently
111 unidentified emissions of organic vapors, particularly chemically complex SVOCs and IVOCs, are vital
112 for advancing the current understanding of the impact of solid fuel combustion on air quality and climate.

113 **2 Materials and methods**

114 **2.1 Fuel and burning types**

115 The experiments were conducted at the Paul Scherrer Institute (PSI) in Villigen, Switzerland. The
116 burning facility is part of the PSI Atmospheric Chemistry Simulation chambers (PACS). Real-time
117 characterization of the primary gas and particle phase emissions was carried out during 28 test burns.

118 Six solid fuels were studied (coal briquettes and biomass fuels: beech logs, spruce/pine logs, fresh
119 spruce/pine branches and needles, dry straw, cow dung) with three to six replicate burns. Material in
120 the beech, spruce, and pine fuels (e.g., logs and needles) was sourced from a local forestry company in
121 Würenlingen, Switzerland. Cow dung cakes (a mixture of cow dung and straw) were collected from
122 Goyla Dairy in Delhi, India. Coal briquettes were purchased from Gansu, China (Ni et al., 2021; Klein
123 et al., 2018).

124 With those six different fuels, we categorized six burning types for this experiment. 1) beech logs stove,
125 2) spruce/pine logs stove, 3) spruce/pine branches and needles open, 4) dry straw open, 5) cow dung
126 open and 6) coal stove. We selected these six solid fuels and conducted emissions tests to simulate
127 certain types of burning found in the atmosphere. Among the list above, 1) beech logs stove and 2)
128 spruce/pine logs stove are representative of residential wood burning, which are burned separately in a
129 stove, consistent with the materials used in two previous articles (Bertrand et al., 2017; Bhattu et al.,
130 2019). To represent forest fires or wildfire and agricultural field combustion, 3) a mixture of fresh
131 spruce/pine branches and needles and 4) straw were combusted in an open stainless-steel cylinder (65
132 cm in diameter and 35 cm in height). Traditional cooking and heating practices in regions like India are
133 represented by 5) cow dung cakes open burning by using half-open stoves (Loebel Roson et al., 2021).
134 Finally, traditional cooking and heating practices in rural regions of developing countries are
135 represented by 6) coal stove burning in a portable cast iron stove purchased from the local market (Liu
136 et al., 2017). Of course, these conditions do not fully accurately represent the conditions found in actual
137 fires, which consist of a variety of burning species (e.g., trees, underbrush, peat soils, etc...), but
138 represent laboratory burning conditions.

139 **2.2 Experimental setup and instrumentation**

140 The experimental design is shown in Figure S1. In summary, it is made up of a burner and a set of
141 diluters with heated lines. The zero air was provided by a zero air generator (737-250 series, AADCO
142 Instruments, Inc., USA) for cleaning and dilution (Heringa et al., 2011; Bruns et al., 2015). The zero air
143 generator takes ambient air and scrubs particulates and volatile organic compounds from the air leaving
144 a mixture that is largely made up of N₂, O₂, and Ar at ambient concentrations. Other trace gases are
145 scrubbed to lower than atmospheric concentrations including CO₂ (< 80 ppb) and CH₄ (< 40 ppb).
146 Before each burn, a continuous stream of zero air was passed through the gas lines overnight to avoid
147 cross-contamination between burns and to ensure a low background of VOCs. Once a burn is initiated
148 from the various combustibles, emissions are sampled from the chimney through a heated line (473 K).
149 The emissions (both gas and particle phases) are then diluted by two Dekati diluters (DI-1000, Dekati
150 Ltd.) which dilutes the emissions by a factor of ~ 100 (473 K, DI-1000, Dekati Ltd.). Note that beech
151 logs combustion cycles consist of a first cycle referred to as the ‘first load’ and subsequent cycles,
152 referred to as ‘reloads’. The first load consisted of a cold start, flaming, smoldering, and burn-out phase,
153 and the reloads were comprised of a warm start, flaming, smoldering, and burn-out phase. Organic
154 vapor emissions of solid fuel combustion are released within 10-30 min after loading according to the
155 properties of the fuels. We define the time until full ignition duration for burning encompasses 80% of
156 the entire process, starting from loading the fuels to burnout.

157 Numerous instruments were connected after the second dekati diluter for the characterization of both
158 the particulate and gaseous phases. A Scanning Mobility Particle Sizer (SMPS, CPC 3022, TSI, and

159 custom-built DMA) provided particle number size distribution information and calibrated by using
160 polystyrene latex (PSL) particle size standards (Wiedensohler et al., 2018; Sarangi et al., 2017). The
161 non-refractory particle composition was monitored by a high-resolution time-of-flight aerosol mass
162 spectrometer (HR-ToF-AMS, Aerodyne Research Inc.). AMS data were processed using SQUIRREL
163 (SeQUential Igor data RetRiEvaL v. 1.63; D. Sueper, University of Colorado, Boulder, CO, USA) and
164 PIKA (Peak Integration and Key Analysis v. 1.23) to obtain mass spectra of identified ions in the m/z
165 range of 12 to 120. OC (organic carbon) is derived from the ratio of organic mass (OM) to OC (OM/OC)
166 determined with high-resolution AMS analysis (Canagaratna et al., 2015). In the AMS mass spectra,
167 the fraction of m/z 60 (f_{60}) represents the ratio of levoglucosan-like species (Schneider et al., 2006;
168 Alfarra et al., 2007). AMS was calibrated for ionization efficiency (IE) by a mass-based method using
169 NH_4NO_3 particles (Tong et al., 2021). Black carbon (BC) was measured with an Aethalometer (Magee
170 Scientific Aethalometer model AE33) (Drinovec et al., 2015) with a time resolution of 1 minute. The
171 maintenance and calibration are given in the AE33 user manual - version 1.57. A LI-7000 CO_2 analyzer
172 (LI-COR) and APMA-370 CO analyzer (Horiba) provided continuous measurements of carbon dioxide
173 (CO_2) and carbon monoxide (CO), respectively. The concentrations of total hydrocarbons (THC) and
174 methane (CH_4) were monitored using a flame ionization detector monitor (THC monitor Horiba APHA-
175 370).

176 We deployed a Vocus to measure organic vapors with a wider range of volatilities. A detailed
177 description of the Vocus is provided elsewhere (Huang et al., 2021; Krechmer et al., 2018). For this
178 study, the Vocus was operated with H_3O^+ as the reagent ion. The sample air was drawn in through a 1
179 m long polytetrafluoroethylene (PTFE) tube (6 mm o.d.) using a total sample flow of 4.3 L/min, which
180 helped reduce the losses in the inlet wall and the sampling delay. Of the total sample flow, only 100-
181 150 cm^3/min went to Vocus, and the rest was exhausted. The Vocus was calibrated before and after
182 measurements every day using a multi-component standard cylinder (Tofwerk AG). Standard gases
183 were diluted by the injection of zero air, producing mixing ratios of VOCs of around 20 ppbv. The
184 calibration components were methanol, acetaldehyde, acetonitrile, acetone, acrylonitrile, isoprene,
185 methyl ethyl ketone, benzene, toluene, m-xylene, α -pinene and 1,2,4-trimethylbenzene. The
186 background measurements were performed using dry zero air every day. Data were recorded with a
187 time resolution of 1 s. The raw data were processed using Tofware v3.2.3 software (TOFWERK,
188 Aerodyne, Inc.). The standard non-targeted analysis workflow developed by Tofwerk was adopted for
189 mass calibration and peak fitting. The mass transmission function and the ratios between the measured
190 and calculated sensitivities for a series of ions were used to quantify the data and convert the ion counts
191 to ppbv. To calculate the mixing ratio for compounds do not present in the calibration mixture, the slope
192 of the linear fit was multiplied by the proton transfer rate constants (k_{ptf}) which have been provided in
193 Supplement Table.

194 **2.3 Data analysis**

195 Modified combustion efficiency (MCE, Equation 1) is an estimate of the relative amount of flaming
196 and smoldering and is equal to

$$MCE = \frac{\Delta \text{CO}_2}{\Delta \text{CO} + \Delta \text{CO}_2} \quad \text{Equation (1)}$$

197 Where ΔCO , ΔCO_2 are the mixing ratios of CO or CO₂ in excess of background (measured before the
 198 combustion), respectively (Christian et al., 2003). Generally, a higher MCE (> 0.9) suggests dominated
 199 flaming combustion, whereas a lower MCE (< 0.9) is mostly associated with smoldering combustion
 200 (Zhao et al., 2021; Zhang et al., 2022).

201 The emission factors (EFs, g kg⁻¹) of species *i* was calculated, following a carbon-mass balance
 202 approach (Andreae, 2019; Boubel et al., 1969; Nelson, 1982):

$$EF_i = \frac{m_i}{\Delta mCO + \Delta mCO_2 + \Delta mCH_4 + \Delta mNMOGs + \Delta mOC + \Delta mBC} \times W_C \quad \text{Equation (2)}$$

203 Here m_i refers to the mass concentration of species *i*. ΔmCO , ΔmCO_2 , ΔmCH_4 , $\Delta mNMOGs$, ΔmOC ,
 204 and ΔmBC are the background-corrected carbon mass concentrations of carbon-containing species in
 205 the flue gas. W_C is the carbon mass fraction of the burning fuel. The W_C in the fuel a constant average
 206 value of 0.46 for wood (Bertrand et al., 2017), 0.45 for straw (Li et al., 2007), 0.45 for cow dung (Font-
 207 Palma, 2019), and 0.49 for coal (Zhang et al., 2000) was assumed. Changes of W_C over the burning
 208 cycle are expected to be small compared to the variability of pollutant emissions. The volatility (i.e. the
 209 saturation mass concentration, C^*) for individual organic compounds was calculated based on the
 210 number of oxygen, carbon, and nitrogen atoms in the compound using the approach by Li et al. (2016):

$$\log_{10} C^* = (n_C^0 - n_C^i) b_C - n_O^i b_O - 2 \frac{n_C^i n_O^i}{n_C^i + n_O^i} b_{CO} - n_N^i b_N \quad \text{Equation (3)}$$

212 where n_C^0 is the reference carbon number; n_C^i , n_O^i and n_N^i denote the numbers of carbon, oxygen, and
 213 nitrogen, respectively, in the compound. b_C , b_O and b_N are the contributions of each atom to $\log_{10} C^*$,
 214 respectively; and b_{CO} is the carbon-oxygen nonideality. The parameters used in this analysis are
 215 presented in Table S1. Most notably, the empirical approach used by Li et al. (2016) was derived with
 216 only a limited number of organonitrates, which could potentially introduce bias in estimating vapor
 217 pressure (Isaacman-Vanwertz and Aumont, 2021). To mitigate this bias, we modified the nitrogen
 218 coefficient for CHON formulas that can be forced to equal twice the negative of the oxygen atom (b_N
 219 = $-2b_O$).

220 2.4 Identification of potential markers

221 In this study, the relative contribution of the mixing ratio for over 1,500 species from six different fuels
 222 was quantified across all 28 test burns using the Vocus. To identify the potential markers of emissions
 223 from different fuels, we implemented the Mann-Whitney U test (Mann and Whitney, 1947; Wilcoxon,
 224 1945) in MATLAB®. Mann-Whitney is a non-parametric test, which has been applied in the selection
 225 of aerosol markers (Zhang et al., 2023), proteomic markers (White et al., 2019; Chen et al., 2012;
 226 Teunissen et al., 2011; Chmaj-Wierzchowska et al., 2015; Nomura et al., 2004), and other biomarkers
 227 (including measurements with a PTR-MS) (Jasperse et al., 2007; Nagai et al., 2020; Sun et al., 2019;
 228 Tritten et al., 2013). It is a nonparametric test and is used for between-group comparisons when the
 229 dependent variable is ordinal or continuous and not assumed to follow a normal distribution with small
 230 sample sizes. This test takes two data samples as parameters, uses the ranks as a measure of central
 231 tendency, and then returns the test results with a *p*-value to indicate the statistical significance. When
 232 the *p*-value is lower than the significance level of 0.1 (a commonly used *p*-value to study statistical
 233 significance in atmospheric research), the median of the tested sample is significantly high or low in

234 the two-tailed test. The molecules from a specific class of fuel that satisfy the pairwise comparison test
235 between one fuel, referred to as fuel j , and other types of fuel, were determined to be significantly high-
236 or low-fraction ions in fuel j . These ions have the potential to serve as potential markers for fuel j . We
237 have calculated in addition the fold change (FC) of ion i in fuel j was calculated using Equation 4,

$$FC_{i,j} = \frac{f_{i,j}}{f_{i,other}} \quad \text{Equation (4)}$$

238 Where $f_{i,j}$ represents the fraction of ion i in the mass spectra profiles of fuel j , and $f_{i,other}$ represents
239 the average fraction of ion i in the mass spectra from the other fuels. For the data used here, the

240 To identify potential markers the Mann-Whitney U test was used to compare the emissions observed
241 for one type of fuel, (e.g., spruce/pine logs) with the gaseous emissions observed for other fuels. The
242 data used for the comparison was the average composition measured throughout a full burning cycle,
243 excluding the initial ignition period. However, due to the similarity in solid fuel types between burning
244 spruce/pine logs, as well as spruce/pine branches and needles, they were categorized as separate solid
245 fuel types for this test and not compared with each other but were only compared with the other four
246 types of fuels. This could result in the loss of many same markers since these two types of fuel actually
247 come from the same type of tree. Therefore, when identifying markers for spruce/pine logs using the
248 Mann-Whitney U test, spruce/pine branches and needles were not included in the comparison group.
249 Similarly, due to the composition of cow dung 'cakes,' which are a mixture of dried cow dung and crop
250 residues, the approach used in the Mann-Whitney U test is consistent with the above method.

251 **3 Results and discussion**

252 **3.1 The characteristics of EF and MCE from different solid fuel types**

253 The average EFs of CO, CO₂, organic vapors and particular matter (PM) in g/kg as well as the MCE
254 values calculated for the 6 types of fuels, are shown in Table 1. Detailed EFs and MCE values for each
255 experiment can be found in Table S2. The average MCE value depends on the solid fuel type and the
256 combustion phase (flaming and smoldering) that is occurring. The lowest MCE values, 0.90, were
257 observed during the smoldering phase of the stove-burning of beech logs, while the highest values (0.99)
258 were recorded during the flaming phase of the spruce/pine branches and needles open burning. In all
259 experiments, the highest EFs for a single gas-phase species correspond to CO₂ (1136.2-1711.7 g/kg).
260 Coal burning has the highest average CO EFs ($40.6 \pm 12.6 \text{ g kg}^{-1}$) and CO₂ EFs ($1680.2 \pm 32.7 \text{ g kg}^{-1}$).

261 Total organic vapor EFs reported in Table 1 refer to species quantified using the Vocus. The average
262 EFs of organic vapors (in the range of 4.8 to 74.2 g kg⁻¹) and the standard deviation are calculated based
263 on the average EFs for the repeatable experiments, which depend on the combustion phases and solid
264 fuel types. Generally, lower MCE values correspond to higher organic vapor EFs within a given class
265 of burning fuel (Figure S2a). For instance, smoldering beech logs resulted in significantly higher
266 average organic vapor EFs ($74.2 \pm 42.9 \text{ g kg}^{-1}$) compared to burning spruce/pine logs. Spruce/pine stove
267 and open burning, dominated by the flaming phase (average MCE > 0.95), exhibited average organic
268 vapor EFs of $44.9 \pm 17.5 \text{ g kg}^{-1}$ and $39.8 \pm 11.4 \text{ g kg}^{-1}$, respectively. This value is higher than previous
269 study (37.3 g kg^{-1}) even though the difference is in the uncertainty levels, which can be attributed to
270 the more extensive analysis of organic vapor in our study (Hatch et al., 2017). Despite the slight

271 difference in MCE for some experiments, the increasing EFs for organic vapors with at least six carbon
272 atoms per molecule ($\geq C_6$) as proxy SOA precursors were observed with lower MCE (Figure S2b)
273 (Bruns et al., 2016). Moreover, the EFs of these SOA precursors are much higher than the primary
274 biomass-burning organic aerosol (BBOA), which suggests a higher potential for SOA formation.
275 Notably, the EFs of organic vapors from cow dung and coal was relatively low, at $4.8 \pm 0.98 \text{ g kg}^{-1}$ and
276 $11.5 \pm 2.6 \text{ g kg}^{-1}$, respectively. Our EFs align well with previously reported volatile organic compound
277 EFs from bituminous coal combustion under similar conditions (range of 1.5 to 14.1 g kg^{-1}) reported by
278 Klein et al. (2018).

279 **3.2 Comparison between flaming and smoldering of wood burning**

280 Figure 1a shows a typical burning cycle during beech log wood experiments with distinct emission
281 characteristics between flaming and smoldering phases. In the top panel, the MCE, CO, and CO₂
282 concentrations, along with our experimental records, are used to indicate the flaming and smoldering
283 stages. The flaming phase shows considerable BC emission, while the smoldering phase is dominated
284 by organic aerosol emissions without visible flame. The absorption Ångström exponent (AAE) during
285 the smoldering phase is approximately twice that of the flaming phase, possibly due to the presence of
286 "brown carbon" in organic aerosols. *f*₆₀ represents the prevalence of primary combustion products such
287 as levoglucosan and is used as an indicator for fresh BB emissions (Schneider et al., 2006; Alfarrá et
288 al., 2007). During the starting/flaming phase, when the temperature is higher, *f*₆₀ increases. Whereas
289 for lower temperatures in the smoldering phase, *f*₆₀ decreases (Weimer et al., 2008). The mixing ratio
290 of most of the compounds correlates negatively with the MCE as expected with a significant increase
291 in the smoldering phase (Figure 1a and Figure S3). However, some compounds like benzene have
292 different enhancement rates from flaming to smoldering, which is similar to previous studies (Warneke
293 et al., 2011).

294 Figure 1b illustrates the measured EFs for flaming and smoldering wood fire stages. On average, EFs
295 for organic vapors in the flaming stage are approximately four times lower ($31.4 \pm 7.1 \text{ g kg}^{-1}$) than those
296 in the smoldering stage fires ($121.9 \pm 24 \text{ g kg}^{-1}$). Despite significant variability in the strength of organic
297 vapors emissions (EFs), the average carbon and oxygen distribution of organic vapors remained largely
298 consistent across the combustion phases (Figure S4). Hardwood (beech) is a fibrous substance primarily
299 composed of three chemical elements: carbon, hydrogen, and oxygen and these basic elements are
300 incorporated into several organic compounds, i.e. cellulose, hemicellulose, lignin, and extractives
301 formed into a cellular structure (Asif, 2009). The flaming stage is associated with more complete
302 oxidation with a relatively higher contribution of oxygenated VOCs (OVOCs, e.g., furan, oxygenated
303 aromatics, O-containing, Figure S5). Conversely, during the smoldering stage, more CO and organic
304 vapors are emitted relative to the flaming stage (Figure 1a). OVOCs, such as carbonyl, furan,
305 oxygenated aromatics, and O-containing species, form the major fraction ($> 88\%$) of emissions in both
306 flaming and smoldering fires. They are followed by the sum of C_xH_y, and SRA (5-10%). As shown in
307 Figure S6, the volatility distribution of the emissions between the flaming phase and smoldering phase
308 changes slightly with a decrease in the IVOCs from 25.8% (flaming) to 20.2% (smoldering). Though,
309 in absolute terms all emissions are enhanced during the smoldering phase, including IVOCs, due to the
310 increased EFs during the smoldering phase. As Figure 1b shows on a relative scale that there is a higher
311 contribution of single ring aromatics and C_xH_y in the smoldering phase than flaming phase. Within these

312 measurements in our residential stove, we observe relatively small differences in the composition
313 relative to the large increase in EFs when moving from flaming to smoldering conditions.

314 **3.3 The characteristics of organic vapor from different solid fuel types**

315 **3.3.1 Chemical composition of organic vapor from combustion**

316 To assess the feasibility of distinguishing differences between combustion solid fuel types based on the
317 measured species, we evaluated the similarity of the mass spectra obtained from each experiment using
318 the correlation coefficient (r), as shown in Figure 2, organic vapors from the same burning fuel are
319 strongly correlated (0.82-0.99), indicating the general repeatability of the experiments. Furthermore,
320 we observed a weak intra-fuel correlation between coal and other biomass sources (0.44-0.78),
321 suggesting significant differences in chemical composition. By contrast, the separation between
322 different solid fuel type is not stark and all possess a correlation between 0.6-0.98. Overall, the
323 correlation coefficient highlights similarities between all biomass-based emissions, which will now be
324 discussed in detail.

325 Figure 2 also shows the average mixing ratio contribution of full ignition duration from m/z 40 to 300
326 for each experiment, and is categorized into C_xH_y , $C_xH_yO_z$, C_xH_yN and $C_xH_yO_zN$ families based on their
327 elemental composition. In all organic vapors, the $C_xH_yO_z$ family is the most abundant group, making
328 the largest contribution to beech logs (88.6%), spruce/pines logs (82.1%) and straw (81.7%). These
329 percentages are higher than those for coal (63.1%) and cow dung (68.9%). Coal burning results in
330 considerably higher contributions in the C_xH_y families (33.7%) than beech logs (9.3%), consistent with
331 the bulk chemical composition of the fuels.

332 Figure 3 separates emitted compounds based on their carbon (x-axis) numbers. The dominant signals
333 in organic vapors for all fuels are attributed to C3-6 compounds, while more species with higher carbon
334 numbers ($\#C > 10$) are observed in spruce/pine branches and needles open burning. The bin containing
335 Hydrogen to carbon ratios (H/C, calculated as the ratio of hydrogen atoms to carbon atoms in a
336 molecules) between 1.2 and 1.5 has the largest contribution in all fuels except the straw, ranging from
337 27% to 31.2%. Oxygen to carbon ratios (O/C, calculated as the ratio of oxygen atoms to carbon atoms
338 in a molecule) less than 0.15 contribute significantly to coal burning (42%), which corresponds to the
339 high proportion of C_xH_y families (Figure 2). Wood and straw burning emitted more oxygenated organic
340 vapors than coal and cow dung burning with more contribution of higher O/C species (O/C > 0.5). The
341 results show similarities to the comparison between burning wood and cow dung in the particle phase
342 (Zhang et al., 2023). Specifically, cow dung exhibits a lower fraction of high O/C (0.22) compared to
343 other fuels studied.

344 We categorized organic vapors by functional groups into 10 classes based on the classifications used in
345 Bhattu et al. (2019). These classes include: alcohols, carbonyls (including acid), hydrocarbons, furans,
346 N-containing compounds, O-containing < 6 (where the number of carbon atoms is less than 6), O-
347 containing ≥ 6 (where the number of carbon atoms is equal or greater than 6), oxygenated aromatics,
348 polycyclic aromatic hydrocarbons (PAHs), single-ring aromatics (SRA). Figure S7 and Figure S8 show
349 a comparison of the organic vapor composition observed from different solid fuel types. The measured
350 emissions exhibit significantly different compositions, reflecting the variability of organic components
351 produced from different solid fuel types. The emissions of all solid fuels are overwhelmingly dominated

352 by carbonyls in the range of 23.1% (coal) to 45.1% (straw). For all emissions, furans represent the
353 second largest group, which account for more than 14% of the emissions. Comparatively, aromatic
354 compounds are less significant in BB: 5.9% - 12% for oxygenated aromatics, 0.5% - 2.1% for PAHs,
355 and 2.1% - 5.8% for SRA. In contrast, aromatic emissions are relatively larger in coal burning emissions
356 (13.6%, 8.1%, and 13.8%, respectively). Also, we note a specific difference in the oxygenated aromatic
357 compounds and those with $C > 6$ for open wood burning conditions, compared to the stove. This
358 difference may be driven by the difference in the water content of the wood, which is significantly
359 higher for open wood burning (30-40%) compared to stove burning (10-12%). The increase in these
360 oxygenated components comes at the expense of species containing carbonyl and furan functionalities.

361 Generally, the total fraction of nitrogen-containing species (C_xH_yN and $C_xH_yO_zN$) is significantly higher
362 in the organic vapors emitted from open burning of cow dung (18.8%) compared to the other fuels (2.1%
363 to 7.3%). This trend is consistent with both our results from aerosol composition measurement and
364 previous literature (Stewart et al., 2021b; Zhang et al., 2023; Loebel Roson et al., 2021). Generally,
365 nitrogen containing compounds in cow dung consist mainly of one nitrogen atom and have a wide range
366 of carbon numbers between 2 and 7 (Figure 3). Stewart et al. (2021a) also reported that cow dung was
367 the largest emitter of nitrogen-containing organic vapors than other fuelwood and crops in India,
368 releasing large amounts of acetonitrile and nitriles. These nitrogen-containing organic vapors are likely
369 formed from the volatilization and decomposition of nitrogen-containing compounds within the cow
370 dung cake, such as free amino acids, pyrroline, pyridine, and chlorophyll (Ren and Zhao, 2015; Burling
371 et al., 2010).

372 **3.2.2 Volatility of organic compounds**

373 The parameterization described in Sect. 2.4 uses the modified approach of Li et al. (2016) to estimate
374 the volatility of each of the measured compounds by the VOCUS in $\log_{10}(C^*)$ [$\mu\text{g m}^{-3}$]. The gaseous
375 organic compounds were grouped into a 14-bin volatility basis set (VBS) (Donahue et al., 2006) (Figure
376 4). Following the suggestions in recent papers (Wang et al., 2024; Li et al., 2023; Donahue et al., 2012;
377 Huang et al., 2021; Schervish and Donahue, 2020), the volatility was aggregated into four main classes
378 with units of $\mu\text{g m}^{-3}$: VOCs as $\log_{10}(C^*) > 6.5$, IVOCs as $\log_{10}(C^*)$ between 6.5 to 2.5, semi-VOCs
379 (SVOCs) as $\log_{10}(C^*)$ between 2.5 to -0.5 and low-VOCs (LVOCs) as $\log_{10}(C^*) < -0.5$).

380 Comparison and compilation of organic vapors sorted by volatility and functional group classification
381 are shown in Figure 4, and the distribution of average EFs as a function of binned saturation vapor
382 concentration is shown. The VOC class was found to be the most abundant, ranging from 58.7% to 87%
383 (Figure S9). For all burning types, carbonyls, furans, and SRA families are overwhelmingly dominant
384 in VOCs, accounting for more than 60% of the VOC emissions. The high fraction of oxygenated VOCs
385 like carbonyls in BB emissions is in stark contrast to VOCs emitted from coal combustion, which is
386 dominated by aromatic hydrocarbon emissions, particularly PAHs. This difference may be attributed to
387 the condensed structure of coal, and lack of oxygen within the fuel itself. PAHs are a group of organic
388 matter compounds containing multiple aromatic rings that mainly result from incomplete combustion
389 (Mastral and Callen, 2000).

390 IVOCs also constituted a considerable fraction in solid-fuel combustions (from 12.6% to 39.3%),
391 particularly in spruce/pine branches and needles (39.3%), cow dung (24.3%) and coal (31.1%) (Figure
392 S9). Significant differences in the bulk volatility of organic compounds were observed among different

393 types of wood burning. In general, spruce/pine branches and needles open burning released a higher
394 proportion of IVOCs (39.3%) into the gas phase compared to stove logs burning (12.6% and 23.9%).
395 This difference may be attributed to a lower percentage of terpenes in woody tissues compared to
396 needle/leaf tissues (Greenberg et al., 2006). In addition, open burning wood has both a significantly
397 larger water content and oxygen content than stove burning, which enhances the formation of partially
398 oxidized organic compounds. Within the open burning experiments, the oxygenated molecules (both
399 aromatics and $C \geq 6$) are enhanced relative to the other experiments and result in the largest EF of
400 IVOCs. In addition to the burning conditions, the fuel properties are also an important factor affecting
401 the IVOC component. Notably, cow dung comprised a higher fraction of N-containing species within
402 their IVOC emissions compared to other fuels. The emissions of IVOCs characterized and quantified
403 in this study are important for the estimating and modeling of aged emissions and their propensity to be
404 able to form secondary organic aerosol.

405 **3.4 Chemical characteristics of dominant compounds from all biomass fuels and** 406 **identification of potential markers for specific solid fuels**

407 **3.4.1 Chemical characteristics of dominant compounds from all biomass fuels**

408 To conduct a comprehensive analysis aimed at identifying potential markers among emissions, the
409 Mann-Whitney U test (refer to Sect. 2.5) was performed on the relative contribution of primary organic
410 vapors derived from various fuels as measured by the Vocus. The results of the pairwise Mann-Whitney
411 test are presented in Figure S10, illustrating the average $-\log_{10} p$ -value as a function of the \log_2 fold
412 change (FC). Species that yield p -values lower than 0.1 in the two-tailed test for all pairwise
413 comparisons are deemed significantly more abundant or scarce in a particular solid fuel type compared
414 to all other fuels. These species are indicated as colored circles in Figure 5. In cases where species do
415 not meet this criterion once or multiple times, they are represented as gray circles, even if their average
416 p -value falls below 0.1. A higher $-\log_{10}(p\text{-value})$ signifies a reduced likelihood that the fractional
417 medians of two species are equivalent. Simultaneously, a greater FC (as per Equation 4) indicates an
418 increased presence of the species' fractional contribution in the tested fuel in comparison to the average
419 contribution across all other fuels. This suggests a higher degree of exclusivity for this species in the
420 given context. The potential markers, p -values, fold changes, and threshold results are listed in the
421 Supplement Table.

422 As shown in Figure 2, biomass fuels (such as logs, branches, needles, straw, and cow dung) were
423 analyzed separately from coal due to their distinct characteristics. To address this distinction, we
424 characterized the dominant compounds across various biomass fuels by setting a threshold (relative
425 mixing ratio contribution $\geq 0.1\%$) for compounds that are not potential markers of one specific biomass
426 fuels. This approach allowed us to identify compounds that are more readily detectable in complex
427 environments. As shown in Figure S11, the gas-phase analysis revealed several dominant compounds:
428 $C_5H_4O_2$ (furfural, 2.2-10.1%), $C_2H_4O_2$ (acetic acid, 2.1-5.8%), $C_3H_6O_2$ (methyl acetate, 1.7-4.6%), and
429 C_2H_4O (acetaldehyde, 1.3-3.9%), which were also reported prior studies on BB (Bruns et al., 2017;
430 Stockwell et al., 2015; Christian, 2004; Sarkar et al., 2016). Furthermore, the category of dominant
431 compounds represents the primary set of compounds associated with BB, contributing from 46% to 69%
432 of the emissions (Figure S12). Carter et al. (2022) expand the representation of fire organic vapors in a
433 global chemical transport model, GEOS-Chem, which contributes substantially to atmospheric

434 reactivity, both locally and globally. Our results could provide more input information for global or
435 regional chemistry transport models.

436 **3.4.2 Identification of potential markers for specific solid fuels**

437 Mass defect plots of potential markers are visualized in Figure 5, for each burning source, respectively.
438 Many potential markers are identified for each unique type of burning (Supplement Table). As shown
439 in Figure 5, potential markers of all wood burning are mainly composed of compounds from the C_xH_y
440 and $C_xH_yO_z$ -family. However, the potential markers for spruce/pine branches and needles have higher
441 molecular weights and are more oxidized, which aligns with their characteristics of the mass spectrum.
442 In contrast, compounds from open burning of straw and cow dung contribute considerably more to
443 nitrogen-containing families but less to oxygen-containing species, consistent with their bulk chemical
444 composition characteristics. Additionally, potential markers for coal consist mainly of compounds from
445 C_xH_y -family, which also aligns with its bulk chemical composition and relatively higher H/C ratios
446 (Figure 3).

447 For all softwood (i.e., spruce/pine logs and spruce/pine branches and needles in this study),
448 monoterpenes ($C_{10}H_{16}$) are a potential marker along with the fragment at m/z 81.07 (C_6H_8). However,
449 monoterpenes cannot exclusively be related to BB given their abundance in the atmosphere.
450 Monoterpenes are also the biogenic volatile organic compounds (BVOCs) emitted from natural trees
451 and other vegetation (Hellén et al., 2012). However, the emission rates of terpenes vary with season,
452 with a higher rate in spring and summer and a lower rate in autumn and winter (He et al., 2000; Noe et
453 al., 2012). In winter, monoterpenes could be a potential marker for softwood burning due to minor
454 natural emissions from spruce, but in summer, terpene emissions from natural trees would dominate the
455 contribution making it a non-potential marker. P-cumenol ($C_9H_{12}O$), as one of the potential markers for
456 beech logs, was discovered to be one of the prominent products of beech wood pyrolysis of lignins
457 (Sengpiel et al., 2019; Keller et al., 2020). Homologues of $C_{10}H_{8-18}O_2$ are determined for spruce/pine
458 branches and needles, with $C_{10}H_{10}O_2$ being β -phenylacrylic acid, which is one of the main chemical
459 compositions of the extract of the cedar pine needle. $C_{10}H_{14}O_2$ could be 1-guaiacylpropane, which is
460 proposed as a potential marker for coniferyl-type lignin pyrolysis products from pine (Simoneit et al.,
461 1993; Liu et al., 2021). Homologues of $C_{11}H_{8-18}O_2$ are also seen, for example, $C_{11}H_{14}O_2$, likely 1-(3,4-
462 dimethoxy-phenyl)-1-propene, which is stated as a representative compound found in lignin (Alves et
463 al., 2003; Hill Bembenic, 2011).

464 Noticeably, cow dung has a significantly different chemical composition. As a result, many potential
465 markers are identified from the burning of cow dung compared to other fuels. These potential markers
466 predominantly contain nitrogen in chemical composition and overlap all potential markers for straw,
467 owing to the mixture of dried cow dung and crop residues in "cow dung cakes." Many nitrogen-
468 containing potential markers are found in straw and cow dung, such as C_4H_5N , C_5H_5N , C_5H_7N , and
469 C_6H_7N , which could likely be assigned to pyrrole, pyridine, methylpyrrole and methyl pyridines
470 respectively. Pyrolysis of the constituents in the crop residue is a probable pathway for these compounds
471 (Ma and Hays, 2008). Acetonitrile (C_2H_3N), acrylonitrile (C_3H_3N), propanenitrile (C_3H_5NO), and 4-
472 methylpentanenitrile ($C_6H_{11}N$) were found as potential markers for cow dung with generally higher FC
473 and higher relative contribution. Additionally, several series of nitrogen-containing homologues are
474 found, such as $C_{10}H_{11-21}NO$, $C_{12}H_{11-21}N$, $C_{11}H_{11-23}NO$ and $C_{15}H_{15-31}N$. These nitrogen-containing gases

475 have also been detected, especially in emissions from cow dung cake in India compared to fuelwood
476 and are likely formed from the volatilization and decomposition of nitrogen-containing compounds
477 within the cow dung cake. These compounds originate primarily from free amino acids but can also
478 arise from pyrroline, pyridine, and chlorophyll (Stewart et al., 2021a).

479 Coal is also a distinct solid fuel compared to other biomass fuels in this study, showing a relatively
480 lower correlation coefficient (Figure 2). Consequently, many series of C_xH_y -family homologues are
481 found. Compounds with 9-12 carbon atoms, as shown in Figure 5 for coal burning, could be PAHs-
482 related, such as C_9H_8 (1-Indene), $C_{10}H_8$ (naphthalene), $C_{10}H_{10}$ (1-methylnaphthalene), $C_{12}H_{10}$
483 (acenaphthene), $C_{12}H_{12}$ (2,6-dimethylnaphthalene). The EFs of the potential markers also show an
484 increasing trend with the decrease of MCE (Figure S13), which suggests EFs of the potential markers
485 are not only dependent upon the type of fuel burnt but also on the burning condition.

486 **4 Conclusions**

487 In this study, we investigated emissions of organic vapors using Vocus during typical solid fuel
488 combustion, including burning of beech logs, spruce/pine logs, spruce/pine branches and needles, straw,
489 and cow dung and coal briquettes. Average EFs of CO, CO₂, organic vapors and PM were calculated.
490 This work provides a comprehensive laboratory-based analysis of the chemical composition of organic
491 vapors emitted from the different combustibles and different combustion phases. We discuss the
492 prominent net combustion emissions from BB and identify new potential markers using the Mann-
493 Whitney U test.

494 The results indicate that wood burning has higher organic vapors EFs compared to other fuels. The
495 emissions varied significantly, ranging from 4.8 to 74.2 g kg⁻¹, depending on the combustion phases
496 and solid fuel types. Despite the slight difference in modified combustion efficiency (MCE) for some
497 experiments, the increasing EFs for organic vapors were observed with lower MCE. Moreover, the EFs
498 of these SOA precursors are much higher than the primary biomass-burning organic aerosol (BBOA),
499 which suggests a higher potential for SOA formation. Distinct particulate/gas emissions at different
500 combustion phases are observed for stove burning of beech logs: initial compositions of flaming or
501 smoldering plumes were dominated by BC or OA, respectively, with much higher organic vapor
502 emission in smoldering. The relative contribution of different classes showed large similarities between
503 the combustion phases in beech logs stove burning, relative to the large change in EFs observed.
504 Therefore, the enhanced EFs under smoldering conditions means there is a greater potential for SOA
505 formation when compared to flaming conditions.

506 The $C_xH_yO_z$ -family is the most abundant group (63.1% to 88.6%) for all solid fuels, followed by C_xH_y
507 (9.3% to 33.7%). A larger contribution of nitrogen-containing species (C_xH_yN and $C_xH_yO_zN$) is found
508 in cow dung burning, while coal burning has a higher contribution from the C_xH_y families. Moreover,
509 the VOC class was found to be the most abundant (58.7% to 87%), followed by the IVOC class (12.6%
510 to 39.3%). Primary semivolatile/intermediate-volatility organic compounds (S/IVOCs) have been
511 proposed as important SOA precursors from BB. Li et al. (2024) found that IVOCs from residential
512 wood burning (~ 13% of total organic vapors) can contribute ~70% of the formed SOA. Overall, these
513 data will help update the IVOC emission inventory and improve the estimates of SOA production.
514 Specifically, these results demonstrate that open burning (e.g., wildfire) emissions have enhanced IVOC

515 EFs, suggesting that the SOA potential from open-burning sources is larger in comparison to their wood
516 stove counterparts.

517 However, each source generally emits a wide spectrum of organic vapors species, leading to
518 considerable overlap between organic vapors species from different sources. Based on the Mann-
519 Whitney U, we selected species that were unique in certain emissions as possible potential markers for
520 specific solid fuels and the dominant compounds for all biomass fuels. Due to minor natural emissions
521 from spruce in summer, monoterpene ($C_{10}H_{16}$) and its fragment could be potential markers for all
522 softwoods (i.e., pine logs and spruce/pine branches and needles in this study) in winter. More products
523 of the pyrolysis of coniferyl-type lignin and the cedar pine needle extract could be found in spruce/pine
524 branches and needles open burning (e.g., $C_{10}H_{14}O_2$, $C_{11}H_{14}O_2$, $C_{10}H_{10}O_2$). The prominent product
525 ($C_9H_{12}O$) resulting from the pyrolysis of beech lignin is identified as the potential markers for beech
526 log stove burning. Many series of nitrogen-containing homologues and nitrogen-containing species (e.g.,
527 acetonitrile, acrylonitrile, propanenitrile, methylpentanenitrile) are identified (e.g., $C_{10}H_{11-21}NO$, $C_{12}H_{11-}$
528 $_{21}N$, $C_{11}H_{11-23}NO$ and $C_{15}H_{15-31}N$), particularly from open burning of cow dung. Coal is a unique solid
529 fuel compared to biomass and more PAHs-related potential markers are identified from coal burning
530 with 9-12 carbon. These potential markers provide important support for future global or regional
531 chemistry transport modeling and source apportionment. Overall, our study provides a comprehensive
532 understanding of the molecular composition and volatility of primary organic compounds, as well as
533 new insights into the identification of potential markers from the burning of solid fuels.

534

535

536

537

538

539

540

541

542

543

544

545

546 **Tables and figures**547 **Table 1** Average EFs of CO, CO₂, organic vapors and PM as well as MCE for 6 types of Solid fuel type.

Solid fuel type	Carbon content	MCE	Emission factors (g kg ⁻¹ fuel)			
			CO	CO ₂	organic vapors	PM
beech logs stove (n=6)	0.46	0.96 ± 0.03	38.9 ± 25.9	1409.4 ± 177.1	74.2 ± 42.9	2.5 ± 1.7
spruce/pine logs stove (n=5)	0.46	0.97 ± 0.01	28.5 ± 14.3	1511.7 ± 68.5	44.9 ± 17.5	1 ± 0.6
spruce/pine branches and needles open (n=3)	0.46	0.99 ± 0.001	2.8 ± 0.8	1579.2 ± 29.7	39.8 ± 11.4	0.9 ± 0.4
straw open (n=4)	0.45	0.97 ± 0.01	24.4 ± 6.6	1488.4 ± 87.2	42.6 ± 33.7	2.8 ± 0.7
cow dung open (n=5)	0.45	0.95 ± 0.03	53.9 ± 27.2	1541.8 ± 50.2	4.8 ± 0.98	1.2 ± 0.61
coal stove (n=5)	0.49	0.96 ± 0.01	40.6 ± 12.6	1680.2 ± 32.7	11.5 ± 2.6	0.9 ± 0.3

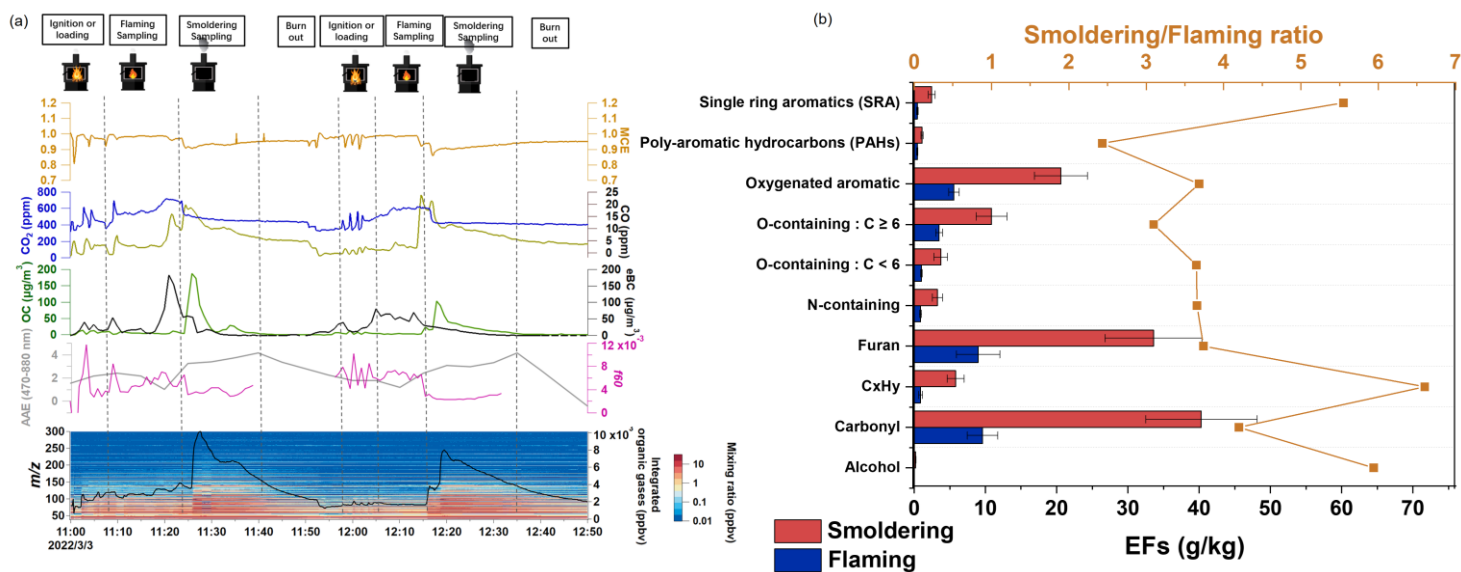
548

549

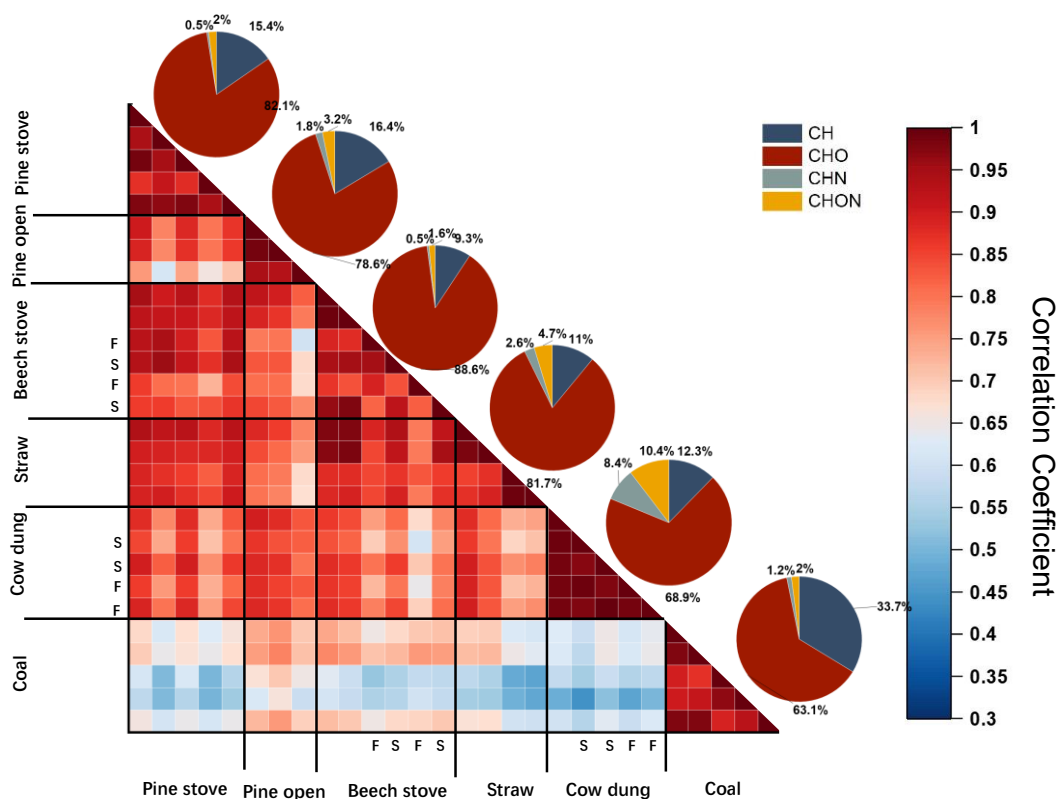
550

551

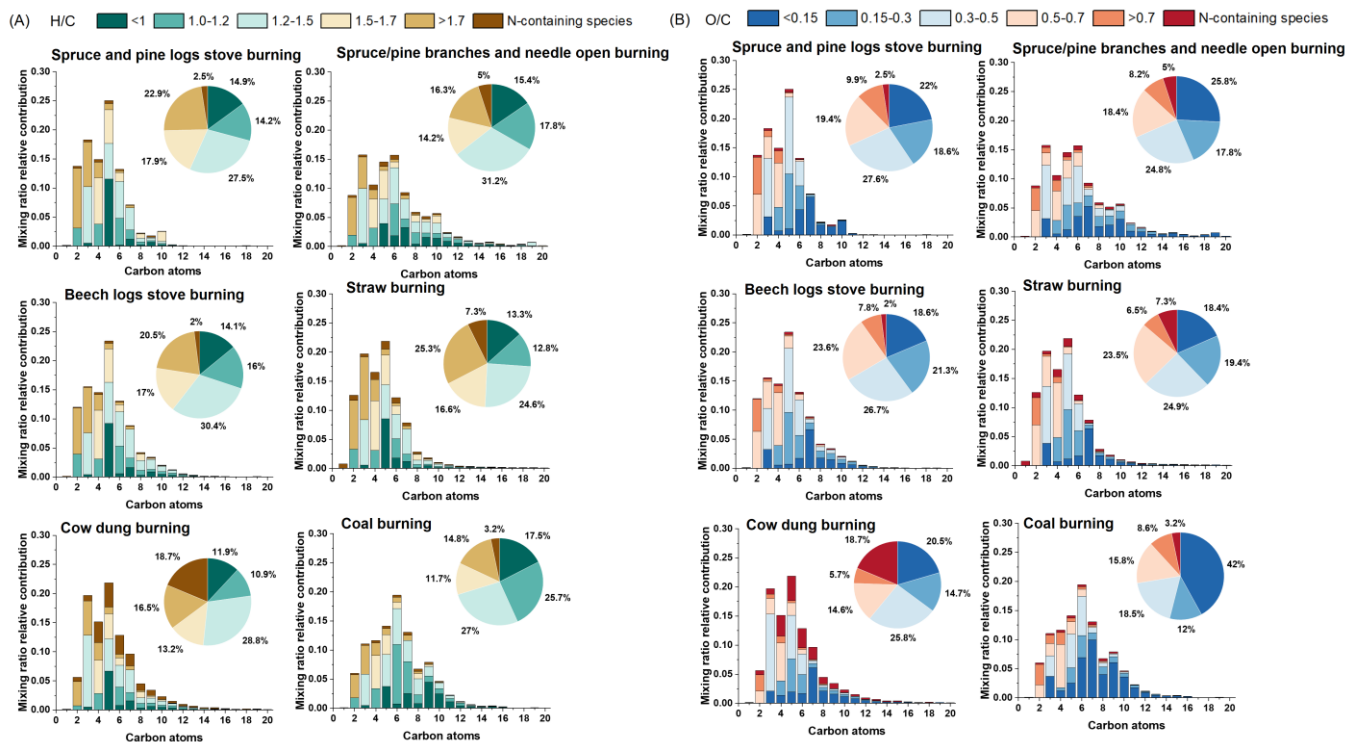
552



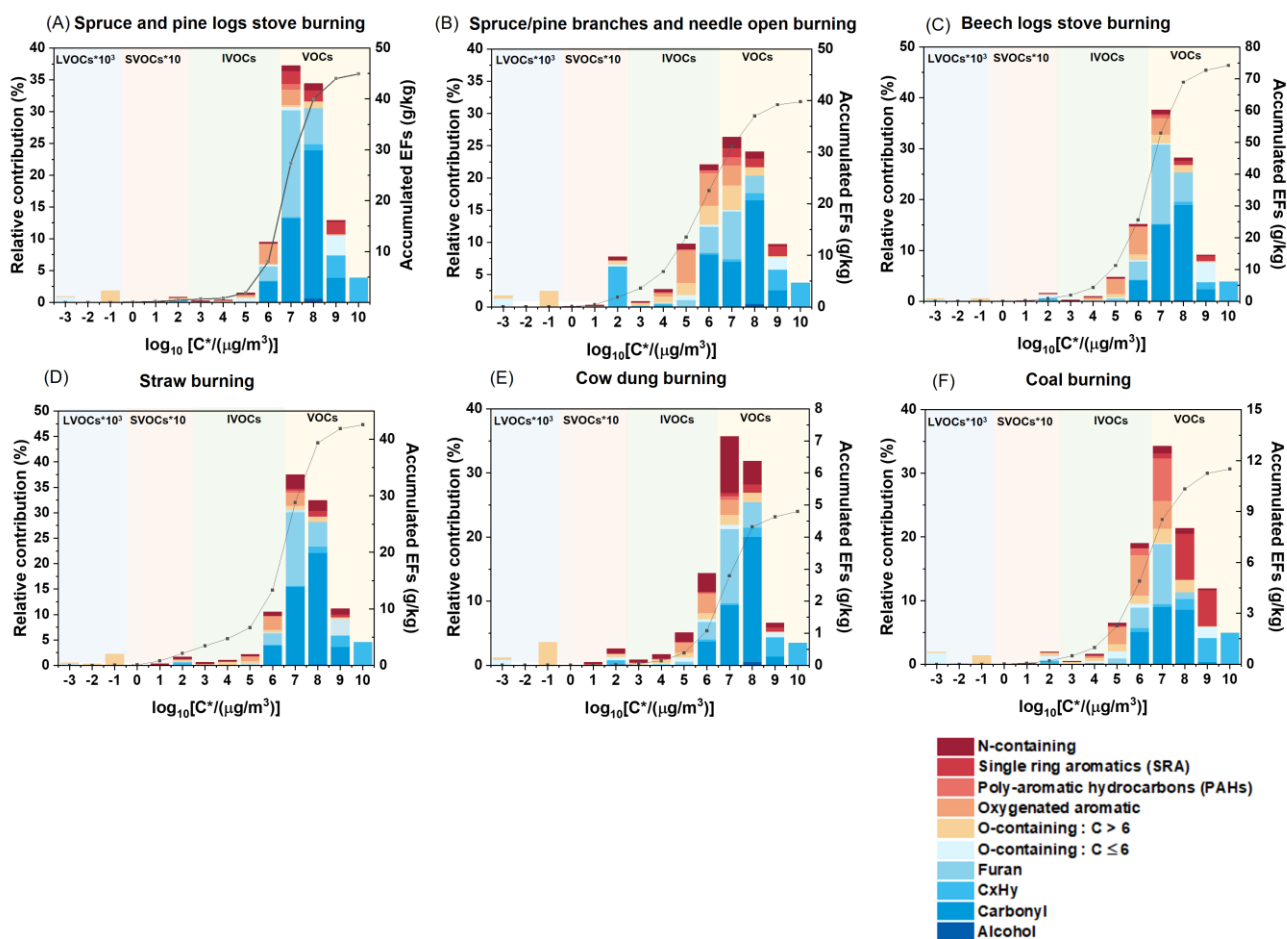
553 **Figure 1.** (a) Temporal profiles of mixing ratios measured by Vocus and evolution of CO, CO₂, AAE, f₆₀, MCE
 554 and key aerosol compositions during burning cycles of beech logs stove burning (b) Geometric mean of the
 555 primary EFs for gas-phase species of different functional groups during flaming and smoldering phase,
 556 respectively (the flaming and smoldering was separated by the experimental record and calculated MCE). Error
 557 bars correspond to the sample geometric standard deviation of the replicates. The square represents the mixing
 558 ratio between smoldering and flaming. In this study, the MCE is used to indicate the flaming stage and smoldering
 559 and a significant decrease of MAC and CO₂ was observed from the flaming phase to the smoldering phase.



561 **Figure 2.** The correlation matrix of organic vapors measured with Vocus (F represents flaming phase and S
 562 represents smoldering phase and unmarked columns and rows represent mixtures of both flaming and smoldering
 563 phases). Pie charts showing the contribution of elemental families are on the diagonal.

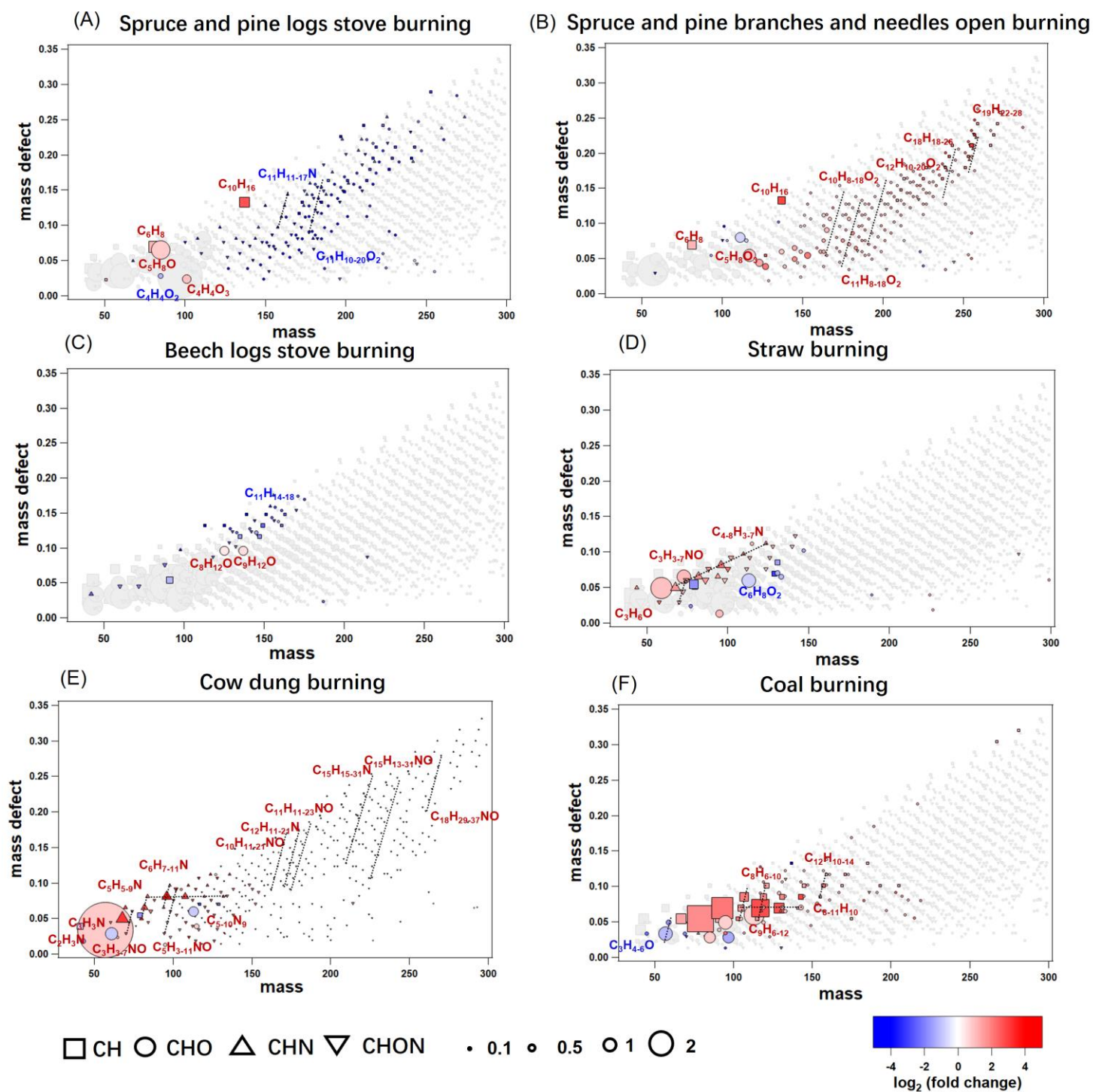


565 **Figure 3.** The average carbon distribution is colored by the H/C (A) and O/C (B) for non-N-containing species.
 566 The pie charts are the corresponding contribution of a range of H/C or O/C ratios.



568 **Figure 4.** Volatility and average accumulated EFs (assume the average molecular weight of each bin are same)
 569 the distribution of primary emissions as a function of binned saturation vapor concentration. Shaded areas indicate
 570 the volatility ranges with units of $\mu\text{g}/\text{m}^3$: VOCs (yellow) as $\log_{10}(C^*) > 6.5$, IVOCs (blue) as $\log_{10}(C^*)$
 571 between 6.5 to 2.5, semi-VOCs (SVOCs, green) as $\log_{10}(C^*)$ between 2.5 to -0.5 and low-VOCs (LVOCs, orange) as
 572 $\log_{10}(C^*) < -0.5$. The relative contribution of LVOCs and SVOCs are multiplied by a factor of 1000 and 10,
 573 respectively.

574



575 **Figure 5.** Mass defect plots identifying potential markers sized by the square root of fractional contribution (%)
 576 and colored by \log_2 (the fold change). The dashed line represents the series of homologues.

577

578

579

580 **Data availability**

581 The data presented in the text and figures are available in the Zenodo online repository (<https://doi.org/10.5281/zenodo.14204572>).

583 **Author contributions**

584 TTW, JZ, HL, KL, RKYC, EG, LK, DMB, and RLM conducted the burning experiments. TTW
585 analyzed the data and wrote the paper. MB, ZCJD, LK, DMB, KL, RLM, IEH, HL, JGS, and ASHP
586 participated in the interpretation of data.

587 **Competing interests**

588 The authors declare that they have no conflict of interest.

589 **Acknowledgments**

590 This work was supported by the Swiss National Science Foundation (SNSF) SNF grant MOLORG
591 (200020_188624), an SNSF Joint Research Project (grant no. IZLCZO_189883), the PSI career return
592 fellowship, and the European Union's Horizon 2020 research, innovation programme under the Marie
593 Skłodowska-Curie grant agreement No 884104 (PSI-FELLOW-III-3i) and ATMO-ACCESS. PSI's
594 atmospheric simulation chamber is a facility of the ACTRIS ERIC and receives funding from the Swiss
595 State Secretariat for Education, Research and Innovation (SERI grant).

596 **Reference**

- 597 Akagi, S., Yokelson, R. J., Wiedinmyer, C., Alvarado, M., Reid, J., Karl, T., Crouse, J., and Wennberg, P.:
598 Emission factors for open and domestic biomass burning for use in atmospheric models, *Atmos. Chem. Phys.*,
599 11, 4039-4072, 2011.
- 600 Akherati, A., He, Y., Coggon, M. M., Koss, A. R., Hodshire, A. L., Sekimoto, K., Warneke, C., de Gouw, J., Yee,
601 L., Seinfeld, J. H., Onasch, T. B., Herndon, S. C., Knighton, W. B., Cappa, C. D., Kleeman, M. J., Lim, C.
602 Y., Kroll, J. H., Pierce, J. R., and Jathar, S. H.: Oxygenated Aromatic Compounds are Important Precursors
603 of Secondary Organic Aerosol in Biomass-Burning Emissions, *Environ. Sci. Technol.*, 54, 8568-8579,
604 10.1021/acs.est.0c01345, 2020.
- 605 Alfarra, M. R., Prevot, A. S., Szidat, S., Sandradewi, J., Weimer, S., Lanz, V. A., Schreiber, D., Mohr, M., and
606 Baltensperger, U.: Identification of the mass spectral signature of organic aerosols from wood burning
607 emissions, *Environmental science & technology*, 41, 5770-5777, 2007.
- 608 Alves, V., Capanema, E., Chen, C.-L., and Gratzl, J.: Comparative studies on oxidation of lignin model
609 compounds with hydrogen peroxide using Mn (IV)-Me3TACN and Mn (IV)-Me4DTNE as catalyst, *J. Mol.*
610 *Catal. A: Chem.*, 206, 37-51, 2003.
- 611 Andreae, M. O.: Emission of trace gases and aerosols from biomass burning—an updated assessment, *Atmos.*
612 *Chem. Phys.*, 19, 8523-8546, 2019.
- 613 Asif, M.: Sustainability of timber, wood and bamboo in construction, in: *Sustainability of construction materials*,
614 Elsevier, 31-54, 2009.
- 615 Bailey, J., Gerasopoulos, E., Rojas-Rueda, D., and Benmarhnia, T.: Potential health and equity co-benefits related
616 to the mitigation policies reducing air pollution from residential wood burning in Athens, Greece, *Journal of*
617 *Environmental Science and Health, Part A*, 54, 1144-1151, 2019.

618 Balakrishnan, K., Ramaswamy, P., Sambandam, S., Thangavel, G., Ghosh, S., Johnson, P., Mukhopadhyay, K.,
619 Venugopal, V., and Thanasekaraan, V.: Air pollution from household solid fuel combustion in India: an
620 overview of exposure and health related information to inform health research priorities, *Global health action*,
621 4, 5638, 2011.

622 Bertrand, A., Stefanelli, G., Bruns, E. A., Pieber, S. M., Temime-Roussel, B., Slowik, J. G., Prévôt, A. S. H.,
623 Wortham, H., El Haddad, I., and Marchand, N.: Primary emissions and secondary aerosol production
624 potential from woodstoves for residential heating: Influence of the stove technology and combustion
625 efficiency, *Atmos. Environ.*, 169, 65-79, 10.1016/j.atmosenv.2017.09.005, 2017.

626 Bhattu, D., Zotter, P., Zhou, J., Stefanelli, G., Klein, F., Bertrand, A., Temime-Roussel, B., Marchand, N., Slowik,
627 J. G., Baltensperger, U., Prevot, A. S. H., Nussbaumer, T., El Haddad, I., and Dommen, J.: Effect of Stove
628 Technology and Combustion Conditions on Gas and Particulate Emissions from Residential Biomass
629 Combustion, *Environ. Sci. Technol.*, 53, 2209-2219, 10.1021/acs.est.8b05020, 2019.

630 Boubel, R. W., Darley, E. F., and Schuck, E. A.: Emissions from burning grass stubble and straw, *Journal of the*
631 *Air Pollution Control Association*, 19, 497-500, 1969.

632 Bruns, E. A., El Haddad, I., Slowik, J. G., Kilic, D., Klein, F., Baltensperger, U., and Prevot, A. S.: Identification
633 of significant precursor gases of secondary organic aerosols from residential wood combustion, *Sci Rep*, 6,
634 27881, 10.1038/srep27881, 2016.

635 Bruns, E. A., Slowik, J. G., El Haddad, I., Kilic, D., Klein, F., Dommen, J., Temime-Roussel, B., Marchand, N.,
636 Baltensperger, U., and Prévôt, A. S. H.: Characterization of gas-phase organics using proton transfer reaction
637 time-of-flight mass spectrometry: fresh and aged residential wood combustion emissions, *Atmos. Chem.*
638 *Phys.*, 17, 705-720, 10.5194/acp-17-705-2017, 2017.

639 Bruns, E. A., El Haddad, I., Keller, A., Klein, F., Kumar, N. K., Pieber, S. M., Corbin, J. C., Slowik, J. G., Brune,
640 W. H., Baltensperger, U., and Prévôt, A. S. H.: Inter-comparison of laboratory smog chamber and flow
641 reactor systems on organic aerosol yield and composition, *Atmos. Meas. Tech.*, 8, 2315-2332, 10.5194/amt-
642 8-2315-2015, 2015.

643 Burling, I., Yokelson, R. J., Griffith, D. W., Johnson, T. J., Veres, P., Roberts, J., Warneke, C., Urbanski, S.,
644 Reardon, J., and Weise, D.: Laboratory measurements of trace gas emissions from biomass burning of fuel
645 types from the southeastern and southwestern United States, *Atmos. Chem. Phys.*, 10, 11115-11130, 2010.

646 Canagaratna, M. R., Jimenez, J. L., Kroll, J. H., Chen, Q., Kessler, S. H., Massoli, P., Hildebrandt Ruiz, L., Fortner,
647 E., Williams, L. R., Wilson, K. R., Surratt, J. D., Donahue, N. M., Jayne, J. T., and Worsnop, D. R.: Elemental
648 ratio measurements of organic compounds using aerosol mass spectrometry: characterization, improved
649 calibration, and implications, *Atmos. Chem. Phys.*, 15, 253-272, 10.5194/acp-15-253-2015, 2015.

650 Carter, T. S., Heald, C. L., Kroll, J. H., Apel, E. C., Blake, D., Coggon, M., Edtbauer, A., Gkatzelis, G., Hornbrook,
651 R. S., and Peischl, J.: An improved representation of fire non-methane organic gases (NMOGs) in models:
652 emissions to reactivity, *Atmos. Chem. Phys.*, 22, 12093-12111, 2022.

653 Chandramouli, C. and General, R.: Census of india 2011, Provisional Population Totals. New Delhi: Government
654 of India, 409-413, 2011.

655 Chen, Y.-T., Chen, H.-W., Domanski, D., Smith, D. S., Liang, K.-H., Wu, C.-C., Chen, C.-L., Chung, T., Chen,
656 M.-C., and Chang, Y.-S.: Multiplexed quantification of 63 proteins in human urine by multiple reaction
657 monitoring-based mass spectrometry for discovery of potential bladder cancer biomarkers, *Journal of*
658 *proteomics*, 75, 3529-3545, 2012.

659 Chmaj-Wierzchowska, K., Kampioni, M., Wilczak, M., Sajdak, S., and Opala, T.: Novel markers in the
660 diagnostics of endometriomas: Urocortin, ghrelin, and leptin or leukocytes, fibrinogen, and CA-125?,
661 *Taiwanese Journal of Obstetrics and Gynecology*, 54, 126-130, 2015.

662 Christian, T. J.: Comprehensive laboratory measurements of biomass-burning emissions: 2. First intercomparison
663 of open-path FTIR, PTR-MS, and GC-MS/FID/ECD, *J. Geophys. Res.*, 109, 10.1029/2003jd003874, 2004.

664 Christian, T. J., Kleiss, B., Yokelson, R. J., Holzinger, R., Crutzen, P., Hao, W. M., Saharjo, B., and Ward, D. E.:
665 Comprehensive laboratory measurements of biomass-burning emissions: 1. Emissions from Indonesian,
666 African, and other fuels, *Journal of Geophysical Research: Atmospheres*, 108, 2003.

667 Donahue, N. M., Kroll, J., Pandis, S. N., and Robinson, A. L.: A two-dimensional volatility basis set–Part 2:
668 Diagnostics of organic-aerosol evolution, *Atmos. Chem. Phys.*, 12, 615-634, 2012.

669 Donahue, N. M., Robinson, A., Stanier, C., and Pandis, S.: Coupled partitioning, dilution, and chemical aging of
670 semivolatile organics, *Environmental science & technology*, 40, 2635-2643, 2006.

671 Font-Palma, C.: Methods for the Treatment of Cattle Manure—A Review, *C*, 5, 10.3390/c5020027, 2019.

672 Font, A., Ciupek, K., Butterfield, D., and Fuller, G.: Long-term trends in particulate matter from wood burning in
673 the United Kingdom: Dependence on weather and social factors, *Environ. Pollut.*, 314, 120105, 2022.

674 Fourtziou, L., Liakakou, E., Stavroulas, I., Theodosi, C., Zarmpas, P., Psiloglou, B., Sciare, J., Maggos, T.,
675 Bairachtari, K., and Bougiatioti, A.: Multi-tracer approach to characterize domestic wood burning in Athens
676 (Greece) during wintertime, *Atmos. Environ.*, 148, 89-101, 2017.

677 Greenberg, J., Friedli, H., Guenther, A., Hanson, D., Harley, P., and Karl, T.: Volatile organic emissions from the
678 distillation and pyrolysis of vegetation, *Atmos. Chem. Phys.*, 6, 81-91, 2006.

679 Grieshop, A., Logue, J., Donahue, N., and Robinson, A.: Laboratory investigation of photochemical oxidation of
680 organic aerosol from wood fires 1: measurement and simulation of organic aerosol evolution, *Atmos. Chem.*
681 *Phys.*, 9, 1263-1277, 2009.

682 Guo, J., Wu, H., Zhao, Z., Wang, J., and Liao, H.: Review on health impacts from domestic coal burning: emphasis
683 on endemic fluorosis in Guizhou Province, Southwest China, *Reviews of Environmental Contamination and*
684 *Toxicology Volume 258*, 1-25, 2021.

685 Hatch, L. E., Rivas-Ubach, A., Jen, C. N., Lipton, M., Goldstein, A. H., and Barsanti, K. C.: Measurements of
686 I/SVOCs in biomass-burning smoke using solid-phase extraction disks and two-dimensional gas
687 chromatography, *Atmos. Chem. Phys.*, 18, 17801-17817, 2018.

688 Hatch, L. E., Yokelson, R. J., Stockwell, C. E., Veres, P. R., Simpson, I. J., Blake, D. R., Orlando, J. J., and
689 Barsanti, K. C.: Multi-instrument comparison and compilation of non-methane organic gas emissions from
690 biomass burning and implications for smoke-derived secondary organic aerosol precursors, *Atmos. Chem.*
691 *Phys.*, 17, 1471-1489, 10.5194/acp-17-1471-2017, 2017.

692 Hatch, L. E., Jen, C. N., Kreisberg, N. M., Selimovic, V., Yokelson, R. J., Stamatis, C., York, R. A., Foster, D.,
693 Stephens, S. L., and Goldstein, A. H.: Highly speciated measurements of terpenoids emitted from laboratory
694 and mixed-conifer forest prescribed fires, *Environmental Science & Technology*, 53, 9418-9428, 2019.

695 He, C., Murray, F., and Lyons, T.: Seasonal variations in monoterpene emissions from Eucalyptus species,
696 *Chemosphere-Global change science*, 2, 65-76, 2000.

697 Hellén, H., Tykkä, T., and Hakola, H.: Importance of monoterpenes and isoprene in urban air in northern Europe,
698 *Atmos. Environ.*, 59, 59-66, 10.1016/j.atmosenv.2012.04.049, 2012.

699 Heringa, M. F., DeCarlo, P. F., Chirico, R., Tritscher, T., Dommen, J., Weingartner, E., Richter, R., Wehrle, G.,
700 Prévôt, A. S. H., and Baltensperger, U.: Investigations of primary and secondary particulate matter of
701 different wood combustion appliances with a high-resolution time-of-flight aerosol mass spectrometer,
702 *Atmos. Chem. Phys.*, 11, 5945-5957, 10.5194/acp-11-5945-2011, 2011.

703 Hill Bembenic, M. A.: The chemistry of subcritical water reactions of a hardwood derived lignin and lignin model
704 compounds with nitrogen, hydrogen, carbon monoxide and carbon dioxide, 2011.

705 Hodzic, A., Jimenez, J. L., Madronich, S., Canagaratna, M. R., DeCarlo, P. F., Kleinman, L., and Fast, J.:
706 Modeling organic aerosols in a megacity: potential contribution of semi-volatile and intermediate volatility
707 primary organic compounds to secondary organic aerosol formation, *Atmos. Chem. Phys.*, 10, 5491-5514,
708 10.5194/acp-10-5491-2010, 2010.

709 Huang, W., Li, H., Sarnela, N., Heikkinen, L., Tham, Y. J., Mikkilä, J., Thomas, S. J., Donahue, N. M., Kulmala,
710 M., and Bianchi, F.: Measurement report: Molecular composition and volatility of gaseous organic

711 compounds in a boreal forest – from volatile organic compounds to highly oxygenated organic molecules,
712 *Atmos. Chem. Phys.*, 21, 8961-8977, 10.5194/acp-21-8961-2021, 2021.

713 Isaacman-VanWertz, G. and Aumont, B.: Impact of organic molecular structure on the estimation of
714 atmospherically relevant physicochemical parameters, *Atmos. Chem. Phys.*, 21, 6541-6563, 10.5194/acp-
715 21-6541-2021, 2021.

716 Jasperse, B., Jakobs, C., Eikelenboom, M. J., Dijkstra, C. D., Uitdehaag, B. M., Barkhof, F., Polman, C. H., and
717 Teunissen, C. E.: N-acetylaspartic acid in cerebrospinal fluid of multiple sclerosis patients determined by
718 gas-chromatography-mass spectrometry, *Journal of neurology*, 254, 631-637, 2007.

719 Jin, L., Permar, W., Selimovic, V., Ketcherside, D., Yokelson, R. J., Hornbrook, R. S., Apel, E. C., Ku, I.-T.,
720 Collett Jr, J. L., and Sullivan, A. P.: Constraining emissions of volatile organic compounds from western US
721 wildfires with WE-CAN and FIREX-AQ airborne observations, *Atmos. Chem. Phys.*, 23, 5969-5991, 2023.

722 Kalogridis, A.-C., Vratolis, S., Liakakou, E., Gerasopoulos, E., Mihalopoulos, N., and Eleftheriadis, K.:
723 Assessment of wood burning versus fossil fuel contribution to wintertime black carbon and carbon monoxide
724 concentrations in Athens, Greece, *Atmos. Chem. Phys.*, 18, 10219-10236, 2018.

725 Keller, R. G., Di Marino, D., Blindert, M., and Wessling, M.: Hydrotropic solutions enable homogeneous fenton
726 treatment of lignin, *Industrial & Engineering Chemistry Research*, 59, 4229-4238, 2020.

727 Klein, F., Pieber, S. M., Ni, H., Stefenelli, G., Bertrand, A., Kilic, D., Pospisilova, V., Temime-Roussel, B.,
728 Marchand, N., El Haddad, I., Slowik, J. G., Baltensperger, U., Cao, J., Huang, R. J., and Prevot, A. S. H.:
729 Characterization of Gas-Phase Organics Using Proton Transfer Reaction Time-of-Flight Mass Spectrometry:
730 Residential Coal Combustion, *Environ. Sci. Technol.*, 52, 2612-2617, 10.1021/acs.est.7b03960, 2018.

731 Koss, A. R., Sekimoto, K., Gilman, J. B., Selimovic, V., Coggon, M. M., Zarzana, K. J., Yuan, B., Lerner, B. M.,
732 Brown, S. S., and Jimenez, J. L.: Non-methane organic gas emissions from biomass burning: identification,
733 quantification, and emission factors from PTR-ToF during the FIREX 2016 laboratory experiment, *Atmos.*
734 *Chem. Phys.*, 18, 3299-3319, 2018.

735 Krechmer, J., Lopez-Hilfiker, F., Koss, A., Hutterli, M., Stoermer, C., Deming, B., Kimmel, J., Warneke, C.,
736 Holzinger, R., Jayne, J., Worsnop, D., Fuhrer, K., Gonin, M., and de Gouw, J.: Evaluation of a New Reagent-
737 Ion Source and Focusing Ion-Molecule Reactor for Use in Proton-Transfer-Reaction Mass Spectrometry,
738 *Anal. Chem.*, 90, 12011-12018, 10.1021/acs.analchem.8b02641, 2018.

739 Kumar, V., Slowik, J. G., Baltensperger, U., Prevot, A. S. H., and Bell, D. M.: Time-Resolved Molecular
740 Characterization of Secondary Organic Aerosol Formed from OH and NO(3) Radical Initiated Oxidation of
741 a Mixture of Aromatic Precursors, *Environ. Sci. Technol.*, 57, 11572-11582, 10.1021/acs.est.3c00225, 2023.

742 Li, H., Riva, M., Rantala, P., Heikkinen, L., Daellenbach, K., Krechmer, J. E., Flaud, P.-M., Worsnop, D., Kulmala,
743 M., Villenave, E., Perraudin, E., Ehn, M., and Bianchi, F.: Terpenes and their oxidation products in the
744 French Landes forest: insights from Vocus PTR-TOF measurements, *Atmos. Chem. Phys.*, 20, 1941-1959,
745 10.5194/acp-20-1941-2020, 2020.

746 Li, K., Zhang, J., Bell, D. M., Wang, T., Lamkaddam, H., Cui, T., Qi, L., Surdu, M., Wang, D., Du, L., Haddad,
747 I. E., Slowik, J. G., and Prevot, A. S. H.: Uncovering the dominant contribution of intermediate volatility
748 compounds in secondary organic aerosol formation from biomass-burning emissions, *National Science*
749 *Review*, 10.1093/nsr/nwae014, 2024.

750 Li, X., Wang, S., Duan, L., Hao, J., Li, C., Chen, Y., and Yang, L.: Particulate and Trace Gas Emissions from
751 Open Burning of Wheat Straw and Corn Stover in China, *Environ. Sci. Technol.*, 41, 6052-6058,
752 10.1021/es0705137, 2007.

753 Li, Y., Pöschl, U., and Shiraiwa, M.: Molecular corridors and parameterizations of volatility in the chemical
754 evolution of organic aerosols, *Atmos. Chem. Phys.*, 16, 3327-3344, 10.5194/acp-16-3327-2016, 2016.

755 Li, Z., Wang, S., Li, S., Wang, X., Huang, G., Chang, X., Huang, L., Liang, C., Zhu, Y., and Zheng, H.: High-
756 resolution emission inventory of full-volatility organic compounds from cooking in China during 2015–2021,
757 *Earth System Science Data*, 15, 5017-5037, 2023.

758 Liu, C., Zhang, C., Mu, Y., Liu, J., and Zhang, Y.: Emission of volatile organic compounds from domestic coal
759 stove with the actual alternation of flaming and smoldering combustion processes, *Environ. Pollut.*, 221, 385-
760 391, 10.1016/j.envpol.2016.11.089, 2017.

761 Liu, Y., Shao, M., Fu, L., Lu, S., Zeng, L., and Tang, D.: Source profiles of volatile organic compounds (VOCs)
762 measured in China: Part I, *Atmos. Environ.*, 42, 6247-6260, 10.1016/j.atmosenv.2008.01.070, 2008.

763 Liu, Y., Liao, B., Guo, W., Fu, Y., Sun, W., Fu, Y., Wang, D., and Kang, H.: Study on Separation and Purification
764 of Chemical Components of Dichloromethane from Pine Needle Extract, *IOP Conference Series: Earth and
765 Environmental Science*, 714, 032039, 2021.

766 Loebel Roson, M., Duruisseau-Kuntz, R., Wang, M., Klimchuk, K., Abel, R. J., Harynuk, J. J., and Zhao, R.:
767 Chemical Characterization of Emissions Arising from Solid Fuel Combustion—Contrasting Wood and Cow
768 Dung Burning, *ACS Earth and Space Chemistry*, 5, 2925-2937, 10.1021/acsearthspacechem.1c00268, 2021.

769 Ma, Y. and Hays, M. D.: Thermal extraction–two-dimensional gas chromatography–mass spectrometry with
770 heart-cutting for nitrogen heterocyclics in biomass burning aerosols, *J. Chromatogr. A*, 1200, 228-234, 2008.

771 Majluf, F. Y., Krechmer, J. E., Daube, C., Knighton, W. B., Dyroff, C., Lambe, A. T., Fortner, E. C., Yacovitch,
772 T. I., Roscioli, J. R., Herndon, S. C., Worsnop, D. R., and Canagaratna, M. R.: Mobile Near-Field
773 Measurements of Biomass Burning Volatile Organic Compounds: Emission Ratios and Factor Analysis,
774 *Environmental Science & Technology Letters*, 9, 383-390, 10.1021/acs.estlett.2c00194, 2022.

775 Mann, H. B. and Whitney, D. R.: On a test of whether one of two random variables is stochastically larger than
776 the other, *Annals of Mathematical Statistics*, 18, 50-60, 10.1214/aoms/1177730491, 1947.

777 Mastral, A. M. and Callen, M. S.: A review on polycyclic aromatic hydrocarbon (PAH) emissions from energy
778 generation, *Environmental Science & Technology*, 34, 3051-3057, 2000.

779 Nagai, K., Uranbileg, B., Chen, Z., Fujioka, A., Yamazaki, T., Matsumoto, Y., Tsukamoto, H., Ikeda, H., Yatomi,
780 Y., and Chiba, H.: Identification of novel biomarkers of hepatocellular carcinoma by high-definition mass
781 spectrometry: Ultrahigh-performance liquid chromatography quadrupole time-of-flight mass spectrometry
782 and desorption electrospray ionization mass spectrometry imaging, *Rapid Commun. Mass Spectrom.*, 34,
783 e8551, 2020.

784 Nelson, R. M.: An evaluation of the carbon balance technique for estimating emission factors and fuel
785 consumption in forest fires, *US Department of Agriculture, Forest Service, Southeastern Forest
786 Experiment ...*1982.

787 Ni, H., Huang, R.-J., Pieber, S. M., Corbin, J. C., Stefanelli, G., Pospisilova, V., Klein, F., Gysel-Beer, M., Yang,
788 L., and Baltensperger, U.: Brown carbon in primary and aged coal combustion emission, *Environmental
789 Science & Technology*, 55, 5701-5710, 2021.

790 Noe, S. M., Hüve, K., Niinemets, Ü., and Copolovici, L.: Seasonal variation in vertical volatile compounds air
791 concentrations within a remote hemiboreal mixed forest, *Atmos. Chem. Phys.*, 12, 3909-3926, 10.5194/acp-
792 12-3909-2012, 2012.

793 Nomura, F., Tomonaga, T., Sogawa, K., Ohashi, T., Nezu, M., Sunaga, M., Kondo, N., Iyo, M., Shimada, H., and
794 Ochiai, T.: Identification of novel and downregulated biomarkers for alcoholism by surface enhanced laser
795 desorption/ionization-mass spectrometry, *Proteomics*, 4, 1187-1194, 2004.

796 Oberschelp, C., Pfister, S., Raptis, C., and Hellweg, S.: Global emission hotspots of coal power generation, *Nature
797 Sustainability*, 2, 113-121, 2019.

798 Permar, W., Wang, Q., Selimovic, V., Wielgasz, C., Yokelson, R. J., Hornbrook, R. S., Hills, A. J., Apel, E. C.,
799 Ku, I. T., and Zhou, Y.: Emissions of trace organic gases from Western US wildfires based on WE-CAN
800 aircraft measurements, *J. Geophys. Res. Atmos.*, 126, e2020JD033838, 2021.

801 Ren, Q. and Zhao, C.: Evolution of fuel-N in gas phase during biomass pyrolysis, *Renewable and Sustainable
802 Energy Reviews*, 50, 408-418, 2015.

803 Riva, M., Rantala, P., Krechmer, J. E., Peräkylä, O., Zhang, Y., Heikkinen, L., Garmash, O., Yan, C., Kulmala,
804 M., Worsnop, D., and Ehn, M.: Evaluating the performance of five different chemical ionization techniques

805 for detecting gaseous oxygenated organic species, *Atmospheric Measurement Techniques*, 12, 2403-2421,
806 10.5194/amt-12-2403-2019, 2019.

807 Robinson, A. L., Donahue, N. M., Shrivastava, M. K., Weitkamp, E. A., Sage, A. M., Grieshop, A. P., Lane, T.
808 E., Pierce, J. R., and Pandis, S. N.: Rethinking organic aerosols: Semivolatile emissions and photochemical
809 aging, *Sci*, 315, 1259-1262, 2007.

810 Sarangi, B., Aggarwal, S. G., and Gupta, P. K.: Performance check of particle size standards within and after
811 shelf-life using differential mobility analyzer, *Journal of Aerosol Science*, 103, 24-37, 2017.

812 Sarkar, C., Sinha, V., Kumar, V., Rupakheti, M., Panday, A., Mahata, K. S., Rupakheti, D., Kathayat, B., and
813 Lawrence, M. G.: Overview of VOC emissions and chemistry from PTR-TOF-MS measurements during the
814 SusKat-ABC campaign: high acetaldehyde, isoprene and isocyanic acid in wintertime air of the Kathmandu
815 Valley, *Atmos. Chem. Phys.*, 16, 3979-4003, 10.5194/acp-16-3979-2016, 2016.

816 Schervish, M. and Donahue, N. M.: Peroxy radical chemistry and the volatility basis set, *Atmos. Chem. Phys.*, 20,
817 1183-1199, 2020.

818 Schneider, J., Weimer, S., Drewnick, F., Borrmann, S., Helas, G., Gwaze, P., Schmid, O., Andreae, M., and
819 Kirchner, U.: Mass spectrometric analysis and aerodynamic properties of various types of combustion-related
820 aerosol particles, *Int. J. Mass spectrom.*, 258, 37-49, 2006.

821 Sengpiel, R., Di Marino, D., Blindert, M., and Wessling, M.: 7 Hydrotropic solutions for Fenton depolymerization
822 of lignin, *Extraction and Electrochemical Valorization of Lignin in Novel Electrolytes*, 107, 2019.

823 Simoneit, B. R., Rogge, W., Mazurek, M., Standley, L., Hildemann, L., and Cass, G.: Lignin pyrolysis products,
824 lignans, and resin acids as specific tracers of plant classes in emissions from biomass combustion,
825 *Environmental science & technology*, 27, 2533-2541, 1993.

826 Stala-Szlugaj, K.: The demand for hard coal for households in Poland and the anti-smog bill, *Archives of Mining
827 Sciences*, 63, 701-711, 2018.

828 Stewart, G. J., Acton, W. J. F., Nelson, B. S., Vaughan, A. R., Hopkins, J. R., Arya, R., Mondal, A., Jangirh, R.,
829 Ahlawat, S., Yadav, L., Sharma, S. K., Dunmore, R. E., Yunus, S. S. M., Hewitt, C. N., Nemitz, E., Mullinger,
830 N., Gadi, R., Sahu, L. K., Tripathi, N., Rickard, A. R., Lee, J. D., Mandal, T. K., and Hamilton, J. F.:
831 Emissions of non-methane volatile organic compounds from combustion of domestic fuels in Delhi, India,
832 *Atmos. Chem. Phys.*, 21, 2383-2406, 10.5194/acp-21-2383-2021, 2021a.

833 Stewart, G. J., Nelson, B. S., Acton, W. J. F., Vaughan, A. R., Farren, N. J., Hopkins, J. R., Ward, M. W., Swift,
834 S. J., Arya, R., Mondal, A., Jangirh, R., Ahlawat, S., Yadav, L., Sharma, S. K., Yunus, S. S. M., Hewitt, C.
835 N., Nemitz, E., Mullinger, N., Gadi, R., Sahu, L. K., Tripathi, N., Rickard, A. R., Lee, J. D., Mandal, T. K.,
836 and Hamilton, J. F.: Emissions of intermediate-volatility and semi-volatile organic compounds from
837 domestic fuels used in Delhi, India, *Atmos. Chem. Phys.*, 21, 2407-2426, 10.5194/acp-21-2407-2021, 2021b.

838 Stockwell, C. E., Veres, P. R., Williams, J., and Yokelson, R. J.: Characterization of biomass burning emissions
839 from cooking fires, peat, crop residue, and other fuels with high-resolution proton-transfer-reaction time-of-
840 flight mass spectrometry, *Atmos. Chem. Phys.*, 15, 845-865, 10.5194/acp-15-845-2015, 2015.

841 Sun, Y., Chen, Y., Sun, C., Liu, H., Wang, Y., and Jiang, X.: Analysis of volatile organic compounds from patients
842 and cell lines for the validation of lung cancer biomarkers by proton-transfer-reaction mass spectrometry,
843 *Analytical Methods*, 11, 3188-3197, 2019.

844 Tao, S., Ru, M., Du, W., Zhu, X., Zhong, Q., Li, B., Shen, G., Pan, X., Meng, W., and Chen, Y.: Quantifying the
845 rural residential energy transition in China from 1992 to 2012 through a representative national survey,
846 *Nature Energy*, 3, 567-573, 2018.

847 Teunissen, C., Koel-Simmelink, M., Pham, T., Knol, J., Khalil, M., Trentini, A., Killestein, J., Nielsen, J., Vrenken,
848 H., and Popescu, V.: Identification of biomarkers for diagnosis and progression of MS by MALDI-TOF mass
849 spectrometry, *Multiple Sclerosis Journal*, 17, 838-850, 2011.

850 Tkacik, D. S., Robinson, E. S., Ahern, A., Saleh, R., Stockwell, C., Veres, P., Simpson, I. J., Meinardi, S., Blake,
851 D. R., Yokelson, R. J., Presto, A. A., Sullivan, R. C., Donahue, N. M., and Robinson, A. L.: A dual-chamber
852 method for quantifying the effects of atmospheric perturbations on secondary organic aerosol formation from

853 biomass burning emissions, *Journal of Geophysical Research: Atmospheres*, 122, 6043-6058,
854 10.1002/2016jd025784, 2017.

855 Tong, Y., Pospisilova, V., Qi, L., Duan, J., Gu, Y., Kumar, V., Rai, P., Stefenelli, G., Wang, L., Wang, Y., Zhong,
856 H., Baltensperger, U., Cao, J., Huang, R.-J., Prévôt, A. S. H., and Slowik, J. G.: Quantification of solid fuel
857 combustion and aqueous chemistry contributions to secondary organic aerosol during wintertime haze events
858 in Beijing, *Atmos. Chem. Phys.*, 21, 9859-9886, 10.5194/acp-21-9859-2021, 2021.

859 Tritten, L., Keiser, J., Godejohann, M., Utzinger, J., Vargas, M., Beckonert, O., Holmes, E., and Saric, J.:
860 Metabolic profiling framework for discovery of candidate diagnostic markers of malaria, *Scientific reports*,
861 3, 2769, 2013.

862 Wang, D. S., Lee, C. P., Krechmer, J. E., Majluf, F., Tong, Y., Canagaratna, M. R., Schmale, J., Prévôt, A. S. H.,
863 Baltensperger, U., Dommen, J., El Haddad, I., Slowik, J. G., and Bell, D. M.: Constraining the response
864 factors of an extractive electrospray ionization mass spectrometer for near-molecular aerosol speciation,
865 *Atmospheric Measurement Techniques*, 14, 6955-6972, 10.5194/amt-14-6955-2021, 2021.

866 Wang, T., Li, K., Bell, D. M., Zhang, J., Cui, T., Surdu, M., Baltensperger, U., Slowik, J. G., Lamkaddam, H.,
867 and El Haddad, I.: Large contribution of in-cloud production of secondary organic aerosol from biomass
868 burning emissions, *npj Climate and Atmospheric Science*, 7, 149, 2024.

869 Warneke, C., Roberts, J. M., Veres, P., Gilman, J., Kuster, W. C., Burling, I., Yokelson, R., and de Gouw, J. A.:
870 VOC identification and inter-comparison from laboratory biomass burning using PTR-MS and PIT-MS, *Int.*
871 *J. Mass spectrom.*, 303, 6-14, 10.1016/j.ijms.2010.12.002, 2011.

872 Weber, K. T. and Yadav, R.: Spatiotemporal trends in wildfires across the Western United States (1950–2019),
873 *Remote Sensing*, 12, 2959, 2020.

874 Weimer, S., Alfarra, M. R., Schreiber, D., Mohr, M., Prévôt, A. S. H., and Baltensperger, U.: Organic aerosol
875 mass spectral signatures from wood-burning emissions: Influence of burning conditions and wood type, *J.*
876 *Geophys. Res.*, 113, 10.1029/2007jd009309, 2008.

877 White, R., Pulford, E., Elliot, D. J., Thurgood, L. A., and Klebe, S.: Quantitative mass spectrometry to identify
878 protein markers for diagnosis of malignant pleural mesothelioma, *Journal of proteomics*, 192, 374-382, 2019.

879 Wiedensohler, A., Wiesner, A., Weinhold, K., Birmili, W., Hermann, M., Merkel, M., Müller, T., Pfeifer, S.,
880 Schmidt, A., and Tuch, T.: Mobility particle size spectrometers: Calibration procedures and measurement
881 uncertainties, *Aerosol Sci. Technol.*, 52, 146-164, 2018.

882 Wilcoxon, F.: Individual Comparisons by Ranking Methods, *Biometrics Bulletin*, 1, 80-83, 10.2307/3001968,
883 1945.

884 Williams, A. P., Allen, C. D., Macalady, A. K., Griffin, D., Woodhouse, C., Meko, D. M., Swetnam, T. W.,
885 Rauscher, S. A., Seager, R., and Grissino-Mayer, H. D.: Temperature as a potent driver of regional forest
886 drought stress and tree mortality, 2012.

887 Wu, D., Zheng, H., Li, Q., Jin, L., Lyu, R., Ding, X., Huo, Y., Zhao, B., Jiang, J., and Chen, J.: Toxic potency-
888 adjusted control of air pollution for solid fuel combustion, *Nature Energy*, 7, 194-202, 2022.

889 Yuan, B., Koss, A. R., Warneke, C., Coggon, M., Sekimoto, K., and de Gouw, J. A.: Proton-Transfer-Reaction
890 Mass Spectrometry: Applications in Atmospheric Sciences, *Chem Rev*, 117, 13187-13229,
891 10.1021/acs.chemrev.7b00325, 2017.

892 Zhang, J. and Smith, K. R.: Household air pollution from coal and biomass fuels in China: measurements, health
893 impacts, and interventions, *Environ. Health Perspect.*, 115, 848-855, 2007.

894 Zhang, J., Li, K., Wang, T., Gammelsæter, E., Cheung, R. K., Surdu, M., Bogler, S., Bhattu, D., Wang, D. S., and
895 Cui, T.: Bulk and molecular-level composition of primary organic aerosol from wood, straw, cow dung, and
896 plastic burning, *Atmos. Chem. Phys.*, 23, 14561-14576, 2023.

897 Zhang, J., Smith, K., Ma, Y., Ye, S., Jiang, F., Qi, W., Liu, P., Khalil, M., Rasmussen, R., and Thorneloe, S.:
898 Greenhouse gases and other airborne pollutants from household stoves in China: a database for emission
899 factors, *Atmos. Environ.*, 34, 4537-4549, 2000.

900 Zhang, X., Xu, J., Zhai, L., and Zhao, W.: Characterization of Aerosol Properties from the Burning Emissions of
901 Typical Residential Fuels on the Tibetan Plateau, *Environ. Sci. Technol.*, 56, 14296-14305,
902 10.1021/acs.est.2c04211, 2022.

903 Zhao, B., Wang, S., Donahue, N. M., Jathar, S. H., Huang, X., Wu, W., Hao, J., and Robinson, A. L.: Quantifying
904 the effect of organic aerosol aging and intermediate-volatility emissions on regional-scale aerosol pollution
905 in China, *Scientific reports*, 6, 28815, 2016.

906 Zhao, N., Li, B., Ahmad, R., Ding, F., Zhou, Y., Li, G., Zayan, A. M. I., and Dong, R.: Dynamic relationships
907 between real-time fuel moisture content and combustion-emission-performance characteristics of wood
908 pellets in a top-lit updraft cookstove, *Case Studies in Thermal Engineering*, 28, 10.1016/j.csite.2021.101484,
909 2021.

910